INFECTIOUS DISEASE

Immune response and clinical severity are shaped by skin-adapted *Staphylococcus aureus* in chronically infected patients

Anne Jamet[1,2]*†, Xiali Fu[1]‡, Céline Dietrich[3]‡, Nathalia Bellon[4,5]‡, Messaouda Attailia[3], Elif Uyar[1], Mélanie Montabord[1], Iharilalao Dubail[1], Khanyisile Kunene[3], Agnès Ferroni[2], Laura Polivka[4,5], Marion Dupuis[1], Daniel Euphrasie[1], Stéphanie Leclerc-Mercier[6], Nathalie Four[3], Ines Metatla[7], Kevin Roger[7], Joanna Lipecka[7], Ida Chiara Guerrera[7], Nicolas Mirouze[8], Alain Charbit[1], Mathieu Coureuil[1], Fabienne Charbit-Henrion[9], Smail Hadj-Rabia[4,5], Julie Steffann[10], Guillaume Lezmi[3,11], Christine Bodemer[4,5]*, Maria Leite-de-Moraes[3]*†

Despite the well-described association of skin lesions with *Staphylococcus aureus*, the distinct ability of clinical isolates to influence the local and systemic inflammatory response in a patient-specific manner is insufficiently characterized. In this study, we analyzed clinical recessive dystrophic epidermolysis bullosa (RDEB), which is characterized by wounds chronically colonized with *S. aureus*, to explore the relationship between inflammatory immune response and strain diversity. Children with RDEB (moderate phenotype, $n = 5$; severe phenotype, $n = 10$) and controls ($n = 18$) were enrolled in the study. Profiling of plasma proteins ($n = 800$), immune cells ($n = 30$ subsets and cytokine-producing cells), and cytokines ($n = 38$) identified a specific inflammatory signature in severe disease. Furthermore, patients with severe RDEB presented a high frequency of interleukin-17A+ (IL-17A+) cells among CD4+ and mucosal-associated invariant T (MAIT) lymphocytes. Positive *S. aureus* cultures from the skin of patients with RDEB allowed whole-genome sequencing of patient strains and assessment of primary keratinocyte immune response upon bacterial challenge. *S. aureus* secretome and conditioned medium from keratinocytes challenged with *S. aureus* strains from patients with severe but not from those with moderate RDEB promoted strong activation and a pro–IL-17 response in both CD4+ and MAIT cells. Our findings show that *S. aureus* strains isolated from patients with severe RDEB induce an IL-17–skewed immune response and pave the way for precision microbiology to explain and predict the highly variable virulence potential of bacterial clinical isolates.

INTRODUCTION

The host immune system is involved in constant dialogue with skin commensal microorganisms while simultaneously preventing the entry of pathogens. This interaction becomes critical when skin integrity is constitutively altered, as in genetic skin diseases associated with recurrent, chronic, nonhealing wounds. MAIT (mucosal-associated invariant T) cells have emerged as key innate-like T cells in the maintenance of homeostasis at mucosal and nonmucosal barriers (*1*, *2*). They represent up to 10% of circulating T cells and are highly abundant within human and mouse skin (*2*, *3*). MAIT cells can produce either type 1 or type 17 cytokines, and they are the dominant interleukin-17A (IL-17A)–producing cells in the human skin (*3*). MAIT cells are unique in expressing an invariant α T cell receptor (TCRα) chain, Vα19-Jα33 (TRAV1-TRAJ33) in mice and Vα7.2-Jα33 (TRAV1.2-TRAJ33) in humans, associated with a limited set of TCRβ chains. Antigen-presenting cells expressing MR1 (major histocompatibility complex class I–related molecule) can activate MAIT cells through the presentation of intermediates of riboflavin biosynthesis (*4*, *5*). These antigenic metabolites are exclusively released by bacteria and fungi including *Staphylococcus aureus*, which is a leading cause of wound infections (*1*, *2*). Alterations in MAIT cell frequencies have been associated with various pathologies, including skin conditions (*2*, *6*–*9*), and a role of MAIT cells in wound healing has been described (*3*, *10*). However, the precise understanding of the functions of MAIT cells remains largely unclear.

Recessive dystrophic epidermolysis bullosa (RDEB) is a rare (incidence estimated at three per million in the US) (*11*) and severe form of genetic mechanobullous disorder (*12*) for which there is currently no curative therapy. RDEB involves a mutation in the *COL7A1* gene, which encodes type VII collagen (C7), resulting in poor epidermal-dermal adherence and skin fragility. Mutations that severely reduce or prevent the production of C7 cause severe forms of the disease with diffuse involvement. Mutations that allow a small amount of normal or partially functional C7 to be produced lead to milder forms. A revised epidermolysis bullosa (EB) classification has been recently

[1]Université Paris Cité, INSERM U1151, CNRS UMR8253, Institut Necker Enfants Malades (INEM), Team Host-Pathogen Integrative Biology, 75015 Paris, France. [2]Department of Clinical Microbiology, Assistance Publique-Hôpitaux de Paris (AP-HP), Hôpital Necker-Enfants Malades, 75015 Paris, France. [3]Université Paris Cité, INSERM U1151, CNRS UMR8253, Institut Necker Enfants Malades (INEM), Team Immunoregulation and Immunopathology, 75015 Paris, France. [4]Department of Dermatology, AP-HP, Hôpital Necker-Enfants Malades, Université Paris Cité, Réseaux national et Européen Maladies rares de la peau FIMARAD et ERN-skin, 75015 Paris, France. [5]Centre de référence MAGEC (Maladies rares de la peau d'origine génétique), IHU Necker Hospital, Imagine Institut, 75015 Paris, France. [6]Department of Pathology, AP-HP, Hôpital Necker-Enfants Malades, 75015 Paris, France. [7]Université Paris Cité, Necker Proteomics, SFR Necker, Inserm US24, 75015 Paris, France. [8]Université de Versailles Saint-Quentin-en-Yvelines, Unité 1173, Laboratoire Infection et Inflammation, 78180 Montigny-le-Bretonneux, France. [9]Laboratory of Medical Genetics, AP-HP, Hôpital Necker-Enfants Malades, Université Paris Cité, 75015 Paris, France. [10]Department of Genomic Medicine for Rare Diseases, Hôpital Necker-Enfants Malades, Université Paris Cité, 75015 Paris, France. [11]Service de Pneumologie et Allergologie Pédiatriques, AP-HP, Hôpital Necker-Enfants Malades, 75015 Paris, France.
*Corresponding author. Email: anne.jamet@inserm.fr (A.J.); Christine.Bodemer@aphp.fr (C.B); maria.leite-de-moraes@inserm.fr (M.L.-d.-M.)
†These authors contributed equally to this work.
‡These authors contributed equally to this work.

proposed (*13*), distinguishing intermediate and severe forms of RDEB. In the most severe forms, not only local but also chronic systemic inflammation is observed. Intriguingly, interindividual differences in patients harboring identical *COL7A1* mutations suggest that environmental factors, such as dysbiosis, could also influence clinical manifestations and disease severity (*14*, *15*). The genetic fragility of the skin of patients with RDEB combined with immune response anomalies (*16*) result in chronic wounds that are chronically infected by *S. aureus* (*17*, *18*). The implication of *S. aureus* in RDEB severity is supported by the correlation of wound burden with *S. aureus* abundance (*19*) and the increased immunoglobulin G (IgG) responses against *S. aureus* antigens observed in patients with EB (*20*). However, the determinants of systemic inflammation and impaired wound healing are poorly understood, and the impact of chronic *S. aureus* skin exposure on the immune systems of patients has not been explored.

In the present study, we investigated the immune and proteomic signatures of children with severe and more moderate forms of RDEB (*13*). We revealed an exacerbated pro–T helper 17 (T_H17) immune response and the role of patients' *S. aureus* strains in altering the host immune response using proteomic, immunological profiling, and in vitro assays. Our results provide a unique example of distinct activation of MAIT cells by *S. aureus* strains harvested from the skin of patients as a function of clinical severity.

RESULTS

Characteristics of patients with RDEB

Patients were selected from the MAGEC (Maladies rares de la peau et des muqueuses d'origine génétique; French national reference center for rare diseases of the skin and mucous membranes of genetic origin) Necker Hospital cohort registering 128 children with RDEB. A total of 15 patients (median age, 7 years; range: 2 to 18 years) with RDEB presenting at the MAGEC during the study period (April to December 2021) were enrolled (Table 1). Five patients with a moderate form of RDEB included one patient with inversa RDEB [EBDASI (Epidermolysis Bullosa Disease Activity and Scarring Index): 57], one patient with localized RDEB (EBDASI: 53), and three patients with intermediate RDEB (EBDASI: 103, 125, and 140). Skin involvement as well as fibrosis and its consequences were limited in all five patients. Patients with inversa RDEB presented with severe oral and esophageal involvement, and the three patients with intermediate RDEB presented with moderate mucosal involvement. The 10 other patients displayed a severe form of RDEB (EBDASI: from 217 to 295). Patients with severe RDEB forms had nonhealing chronic wounds, severe mucosal damage, and severe fibrosis with important functional impairment. No history of carcinoma was observed in this pediatric RDEB cohort. Diagnosis was confirmed by the clinical presentation, the extent of cleavage (the specific plane of skin separation occurring below the lamina densa in RDEB), and immunostaining of skin samples for all patients. The identification of mutations in the *COL7A1* gene was available for 14/15 patients. Hereafter, patients are designated as having moderate (intermediate, localized, or inversa; $n = 5$) or severe RDEB ($n = 10$). Representative clinical images of patients with moderate and severe RDEB forms and COL7A1 immunostaining are shown in fig. S1 (A and B). In addition, 18 age-matched children without a skin disorder and a control group of 8 females and 10 males 5.0 [3.75 to 9.25] years old were included. Blood samples were obtained from all of the patients ($n = 15$) and controls ($n = 18$) to perform untargeted proteomic and cytokine profiling from plasma as well as for immunophenotyping of circulating immune cell populations. On the same day, we obtained skin samples from the 10 patients with severe and 3 patients with moderate RDEB for selective detection and semiquantification of *S. aureus* (fig. S1C). Skin samples were collected from patients following the routine procedure of the dermatology department using ESwabs (Copan); these samples were sent to the Necker Hospital clinical microbiology laboratory for processing within 2 hours of collection.

Immune cell profiling reveals major differences in T and B cell populations in patients with RDEB

Fresh peripheral blood mononuclear cells (PBMCs) were stained with distinct markers to identify the major T cell populations among

Table 1. General and clinical characteristics of the patients with RDEB. NA, not applicable.

Patients	Age (year)	Sex	Clinical manifestation	Immunostaining—collage VII	EBDASI score	*S. aureus* load (0 to 8)
RDEB159	16	M	Inversa	Absent	67/506	NA
RDEB101	16	M	Intermediate	Positive	103/506	NA
RDEB181	2	F	Intermediate	Positive	140/506	1
RDEB156	9	M	Localized	Positive	53/506	1
RDEB150	3	M	Intermediate	Positive	125/506	1
RDEB069	6	F	Severe	Positive	295/506	3
RDEB148	7	F	Severe	Positive	217/506	3
RDEB071	7	M	Severe	Low staining	217/506	8
RDEB163	3	F	Severe	Positive	223/506	6
RDEB076	18	F	Severe	Absent	221/506	1
RDEB168	14	F	Severe	Absent	276/506	2
RDEB093	4	F	Severe	Absent	228/506	5
RDEB055	6	F	Severe	Absent	303/506	4
RDEB056	6	F	Severe	Absent	270/506	4
RDEB158	14	M	Severe	Absent	225/506	2

gated conventional CD4+ and CD8+ T cells and MAIT cells (defined as CD3+CD161+MR1-5-OP-RU+ tetramers) (fig. S2). We found no major differences in the frequencies of CD4+, CD8+, or MAIT cells between the moderate RDEB, severe RDEB, and control groups (table S1).

To test the cytokine-producing capacities of these distinct T cell populations, PBMCs were cultivated for 5 hours in the presence of phorbol 12-myristate 13-acetate (PMA) plus ionomycin and analyzed for production of IL-4, IL-13, IL-17A, interferon-γ (IFN-γ), and tumor necrosis factor–α (TNFα). An example of staining of cytokine production among gated conventional CD4+ and CD8+ T cells and MAIT cells is presented in fig. S3. The frequencies of IL-17A–producing CD4+ T cells were significantly higher in the moderate ($P = 0.0369$) and severe ($P = 0.0004$) RDEB groups compared with the control group (Fig. 1A and table S1). Concerning MAIT cells, we found that IL-17A–producing MAIT (or MAIT17) cells were enhanced in patients with severe RDEB compared with controls (Fig. 1A). No substantial differences concerning IL-4, IL-13, IFN-γ, or TNFα production by MAIT, CD4+, and CD8+ T cell subsets, nor IL-17A production by CD8+ T cells, were observed between the groups (table S1). These findings suggest that severe RDEB presents with a skewed pro-T_H17 immune response.

Identification of the plasma immune signature in patients with RDEB

Compared with control donors, patients with severe RDEB had higher plasma concentrations of 14 of the 38 cytokines measured (Fig. 1B and table S2). Pro-T_H2 (IL-4 $P = 0.0003$ and IL-9 $P = 0.0036$), pro-T_H17 (IL-17A $P = 0.0011$, IL-17F $P = 0.0058$, and IL-22 $P = 0.0027$), and proinflammatory cytokines [IL-2 $P = 0.0029$, IL-6 $P < 0.0001$, IL-8 $P = 0.0041$, IL-33 $P = 0.0427$, TNFα $P = 0.0005$, TSLP (thymic stromal lymphopoietin) $P = 0.0006$, ENA-78 (epithelial neutrophil-activating protein 78) $P = 0.0129$, MIP-3α (macrophage inflammatory protein-3α) $P = 0.0002$, and GROα (growth-regulated oncogene α) $P < 0.0001$] were significantly higher in patients with severe RDEB compared with controls (Fig. 1B), and MIP-3α was also higher in patients with severe RDEB compared with moderate RDEB ($P = 0.0002$) (Fig. 1B). The plasma concentration of ENA-78 was also significantly higher in patients with moderate RDEB than in controls ($P = 0.0478$) (Fig. 1B). Overall, cytokine production was detected in most patients, whereas IL-4, IL-8, IL-17A, IL-17F, and TSLP were detected in only a few of the controls (Fig. 1B).

We further asked whether there was a preferential correlation between the high concentrations of cytokines found in patients with RDEB. A multiparametric matrix correlation plot showed that most cytokines strongly positively correlated with each other (Fig. 1C). A particular core of cytokines was more highly correlated among themselves, comprising IL-2, IL-4, IL-5, IL-9, IL-10, IL-13, IL-17F, IL-22, IFN-γ, and TNFα from one side and IL-17A, IL-33, TSLP, IL-1β, IL-8, IL-11, IL-12p40, IL-12p70, IL-16, IL-23, IL-27, granulocyte-macrophage colony-stimulating factor (GM-CSF), IFN-α2, IL-1α, IP-10, MIP-1α, MIP-1β, and monokine induced by interferon gamma (MIG) from the other side (Fig. 1C). A negative correlation was observed only with RANTES (Fig. 1C). Plasma cytokine concentrations in controls showed fewer correlations (Fig. 1D). Together, these data suggest that inflammatory processes in patients with RDEB involve concomitant activation of distinct proinflammatory cytokines but with a preference for the pro-T_H17 profile.

A proteomic signature distinguishes patients with RDEB from control donors

We undertook an untargeted proteomic approach on plasma from patients and controls to define their respective proteomic signature. We carried out workflow optimization of neat plasma analysis using the dia-PASEF (data-independent acquisition–parallel accumulation-serial fragmentation) approach to maximize the number of protein groups identified and quantified while minimizing both gradient time and missing value concentrations (fig. S4). We were able to identify up to 1352 proteins. Of these, 829 were considered eligible for statistical analysis (fig. S4). Significantly different proteins between groups are shown in data file S1, and the full list of proteins is provided as dataset PXD042141 in the PRIDE repository.

Partial least squares–discriminant analysis (PLS-DA) revealed a distinct separation between patients with severe RDEB and controls, whereas patients with moderate RDEB were intermediate between patients with severe RDEB and controls (Fig. 2A). Among the 829 proteins quantified, 297 of the most differentially expressed proteins (DEPs) were identified in our comparison of all patients with controls, of which 129 were up-regulated and 168 were down-regulated (Fig. 2B and data file S1). The top five significantly enriched Gene Ontology (GO) terms in biological process (BP), cellular component (CC), and molecular function (MF) categories among the down-regulated DEPs in patients compared with controls were associated with extracellular matrix (ECM structural constituents and ECM organization) and wound healing (Fig. 2C). ECM pathways included extracellular structure organization, collagen metabolic process, and regulated exocytosis. Of note, the most-enriched GO term among down-regulated DEPs was "collagen-containing extracellular matrix" (Fig. 2C).

The most-enriched GO terms among the up-regulated DEPs in patients with RDEB compared with controls were mainly involved in biological processes associated with immune response (for example, "antigen binding," "immunoglobulin production," and "complement activation") and hemostasis (Fig. 2D). Immune response includes humoral immune response, leukocyte migration, acute-phase response, and initial triggering of complement. Hemostasis includes the formation of a fibrin clot (clotting cascade) and complement and coagulation cascades.

The most-notable up-regulated proteins involved in inflammation were CRP (complement-reactive protein), SAA1 (serum amyloid A-1 protein), SAA2 (serum amyloid A-2 protein), NRCAM (neuronal cell adhesion molecule), and S100A 8 and 9 (protein S100A) (Fig. 3A). In parallel, down-regulated proteins involved in cell adhesion included DPT (dermatopontin), ITGA2 (integrin alpha-2), POSTN (periostin), LAMB1 (laminin subunit beta-1), and CDH13 (cadherin-13) (Fig. 3A). Proteins involved in extracellular proteolysis and tumor invasion such as SERPINA 1, 3, 4, 5, and 6 (plasma serine protease inhibitor), FETUB (fetuin-B), and CLEC3B (tetranectin) were also decreased in patients with severe RDEB compared with controls (Fig. 3A and data file S1).

Patients with severe RDEB exhibit an *S. aureus* infection signature and deregulation of IL-17 pathways

Whereas 297 DEPs (293 with gene names) were found to be significantly different between patients with severe RDEB and controls, only 3 DEPs were found between patients with severe versus intermediate RDEB (SAA1 $P = 0.020$, SAA2 $P = 0.018$, and NRCAM $P = 0.018$). In addition, six DEPs were found between patients with

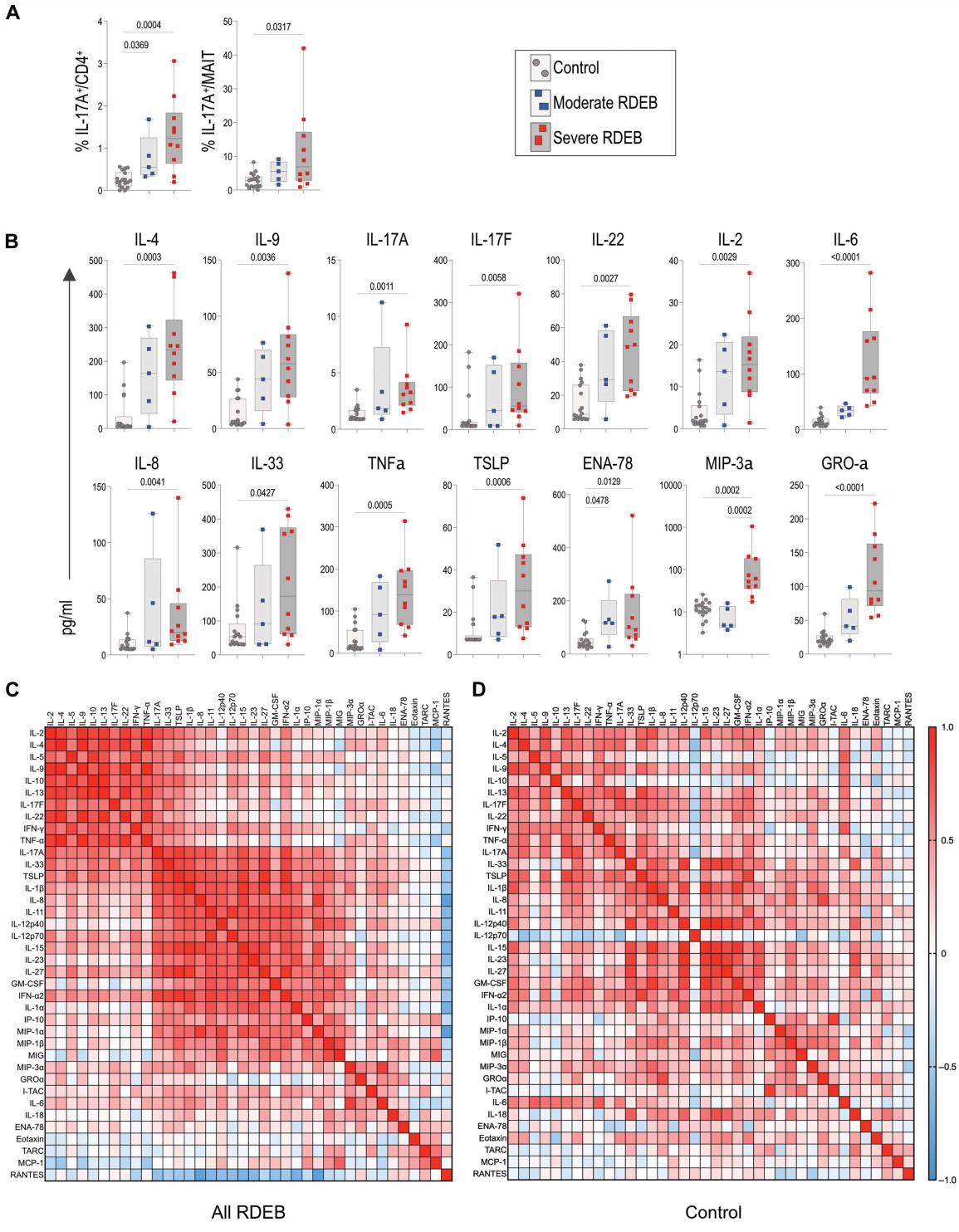

Fig. 1. Circulating immune cell profiling. (**A**) Frequencies of IL-17A+ among gated conventional CD4+ and MAIT cells in control individuals ($n = 18$) and patients with moderate RDEB ($n = 5$) or severe RDEB ($n = 10$). (**B**) Concentrations of 14 proinflammatory cytokines/chemokines in the plasma showing higher quantities in patients with severe RDEB compared with controls. Data indicate the medians. Each point within the box plot represents one individual. Statistical differences were determined by the Kruskal-Wallis test with Benjamini-Hochberg corrections. Significant q values ($q < 0.05$) are indicated. (**C** and **D**) Multiparametric matrix correlation plot of cytokine concentrations in patients with RDEB ($n = 15$) (C) and controls ($n = 18$) (D).

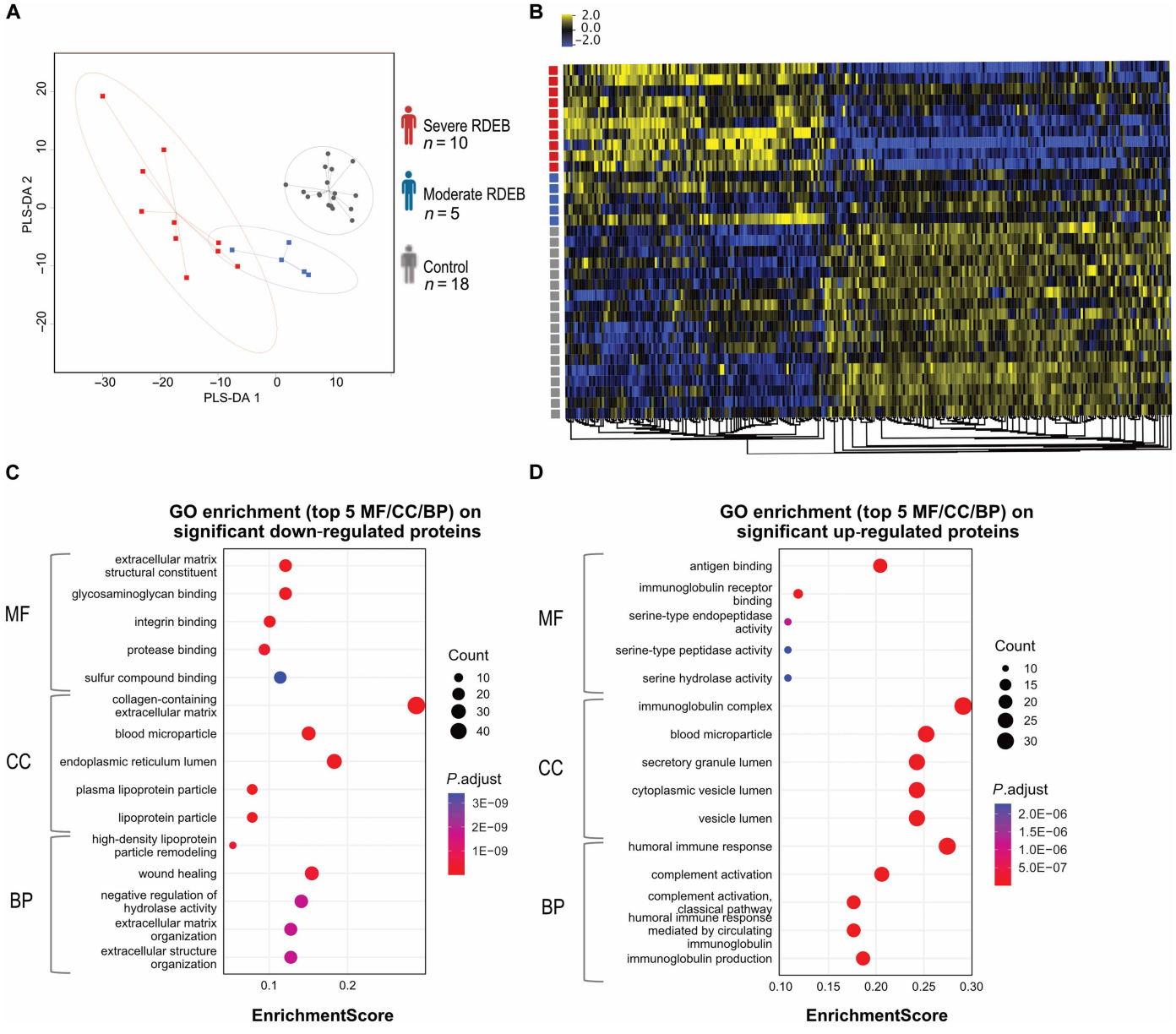

Fig. 2. Global view of plasma proteomic profiling. (**A**) Graph of the individuals provided by PLS-DA modeling showing the ability of plasma proteomic profiling to distinguish patients with severe RDEB (n = 10), those with moderate RDEB (n = 5), and control individuals (n = 18). (**B**) Heatmap and hierarchical clustering of significantly deregulated proteomic data revealed separation between patients with severe RDEB, those with moderate RDEB, and control individuals. (**C**) GO enrichment analysis of the significantly down-regulated proteins showing enrichment in proteins associated with ECM in patients with RDEB compared with controls. (**D**) GO enrichment analysis of the significantly up-regulated proteins showing enrichment in proteins associated with immune response in patients with RDEB compared with controls. The bubble size indicates the number of proteins, and the color bar indicates the adjusted P values.

intermediate RDEB versus controls [CFHR5 (complement factor H-related protein 5) $P = 0.0153$, DPP4 (dipeptidyl peptidase 4) $P = 0.037$, LRG1 (leucine-rich alpha-2-glycoprotein) $P = 0.0138$, NCAM1 (neural cell adhesion molecule 1) $P = 0.0261$, BASP1 (brain acid soluble protein 1) $P = 0.0210$, and CPB2 (carboxypeptidase B2) $P = 0.045$] (Fig. 3A). KEGG (Kyoto Encyclopedia of Genes and Genomes) pathway analysis conducted on the 293 proteins distinguishing patients with severe RDEB from controls showed "complement and coagulation cascades," "ECM-receptor interaction," and "*Staphylococcus aureus* infection" (pathway hsa05150) among the top 10 enriched pathways (Fig. 3B). We observed that SAA1 was negatively correlated with SERPINA5 and FETUB (Fig. 3, C and D), as previously shown by proteomic analysis of sera from patients with *S. aureus* bacteremia (*21*). Moreover, CLEC3B (tetranectin), a serum protein known to be depleted in patients with sepsis (*22*), was also down-regulated in patients with RDEB (Fig. 3A). In contrast, IL-17–regulated antimicrobial peptides belonging to the S100 protein family (S100A8 and S100A9) were up-regulated in patients with severe RDEB (Fig. 3A). Furthermore, a positive correlation was observed between IL-17F and S100A8 as well as S100A9 (Fig. 3, E and F). Together, these findings

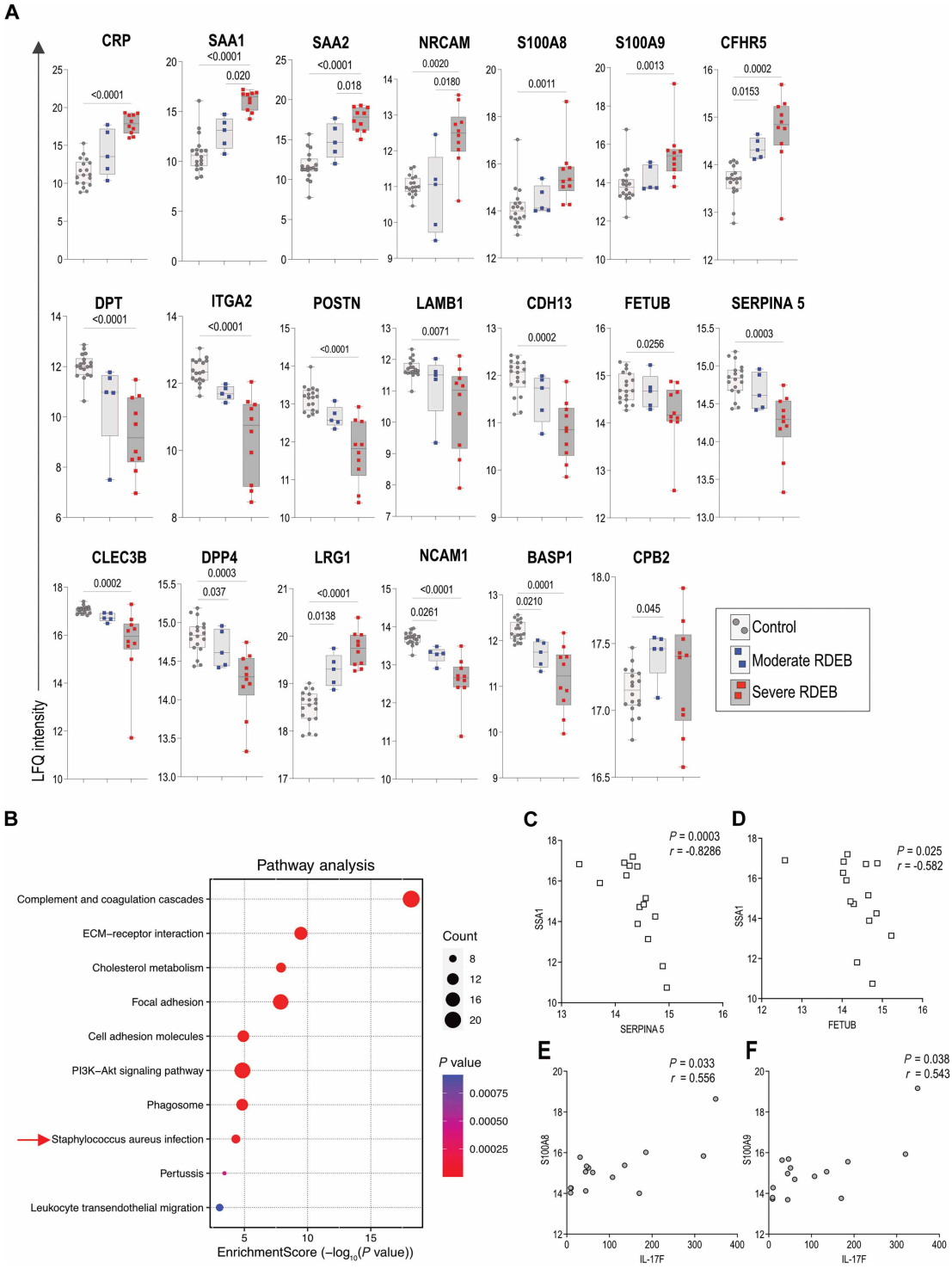

Fig. 3. Plasma proteomic profiling analysis. (**A**) Box-and-whisker plots showing top DEPs as well as selected proteins in patients with severe RDEB ($n = 10$) compared with patients with moderate RDEB ($n = 5$) and controls ($n = 18$). Data indicate the medians. Each point within the box plot represents one individual. Statistical differences were determined by the Kruskal-Wallis test with Benjamini-Hochberg corrections. Significant q values ($q < 0.05$) are indicated. LFQ, label-free quantification. (**B**) Pathway enrichment analysis of DEPs in patients with severe compared with moderate RDEB. The bubble size indicates the number of proteins, and the color bar indicates the adjusted P values. (**C** to **F**) Spearman correlation between SAA1 and SERPINA5 (C) or FETUB (D) and between IL-17F and S100A8 (E) or S100A9 (F) concentrations in the plasma of patients with RDEB. Each point represents one patient. $P < 0.05$ was considered as significant.

suggest a potential contribution of *S. aureus* in shaping the plasma proteomic profile of patients with severe RDEB.

S. aureus load and strain genotype diversity in patients

The skin pathogen *S. aureus* is well known to colonize patients with RDEB (*19*). Our proteomic profiling of patients with severe RDEB showed a signature of the host response to infection that was consistent with a response to *S. aureus*. In 13 patients with RDEB, microbiological skin samples were taken using ESwabs (Copan) on the same day as the blood tests, which made it possible to assess the *S. aureus* load and the *S. aureus* strain genotypes (Fig. 4A).

All sampled patients harbored *S. aureus* in at least one of the two sampled sites. Sequencing revealed that the 13 patient strains belonged to nine sequence types (STs) (Fig. 4B), in line with the lack of a specific ST associated with RDEB (*23*). For two patients (RDEB076 and RDEB168), we had a previous microbiological sampling available, allowing us to sequence *S. aureus* strains collected 1 to 2 years earlier. For those two patients, the two earlier strains belonged to the same clone as the latter strains, showing the persistent colonization by a predominant clone (Fig. 4B). The *S. aureus* load was significantly higher in patients with severe compared with moderate RDEB ($P = 0.0245$) (Fig. 4C) and positively correlated with the concentrations of IL-17F, GROα, and I-TAC (interferon-inducible T cell alpha chemoattractant) detected in the plasma (Fig. 4, D to F), suggesting a possible relationship between *S. aureus* and proinflammatory cytokines in patients with RDEB.

Secreted proteins of *S. aureus* patient strains contribute to their ability to trigger an inflammatory response in keratinocytes

To investigate the impact of *S. aureus* clinical strains on the inflammatory response, we challenged primary keratinocytes with secretomes of *S. aureus* collected from patients and the corresponding conditioned medium (CM) was used to assess the cytokine released. Of note, all of the clinical isolates grew equally well in the culture medium (fig. S5). We first found two cytokine response profiles upon *S. aureus* stimulation with either a low or high amount of inflammatory cytokine production (IL-1α, IL-6, IL-8, IL-11, IL-12p70, IL-15, IL-18, IL-23, IL-27, IL-33, TNFα, GROα, and GM-CSF) (Fig. 4G). The three strains collected from patients with moderate RDEB (strains hereafter named as Sa-moderate) exhibited low production of inflammatory cytokines as compared with strains from patients with severe RDEB (Sa-severe) (Fig. 4G). For the two patients for whom we obtained earlier isolates, we showed that the earlier isolates had a similar ability to stimulate primary keratinocytes (Fig. 4H), supporting a possible long-term impact on the host immune response of persistent *S. aureus* clones.

S. aureus strains from patients with severe RDEB trigger a pro–IL-17 inflammatory response in PBMCs

To further test the ability of *S. aureus* clinical strains to affect immune response, we performed immune cell profiling upon PBMC stimulation with bacterial secretome (BS) and CM obtained by the stimulation of primary keratinocytes with *S. aureus* strains from patients with moderate RDEB (hereafter named as BS and CM Sa-moderate, $n = 3$) and selected patients with severe RDEB (hereafter named as BS and CM Sa-severe, $n = 4$) (Fig. 5A). The four *S. aureus* strains from patients with severe RDEB were selected according to their ability to stimulate primary keratinocytes (Fig. 4G). We focused our attention on CD4+ and MAIT cells and pro-T_H17 cytokines. BS Sa-severe induced higher activation of MAIT and CD4+ cells (determined by CD69 expression) as compared with BS Sa-moderate and control medium (Fig. 5B). Similarly, the frequency of IL-17A+ among gated MAIT and CD4+ T cells was higher in response to BS Sa-severe than to BS Sa-moderate or control medium (Fig. 5B). No notable difference was observed when CD8+ T cells were analyzed (fig. S6, A and B).

Likewise, CM Sa-severe induced higher activation of MAIT and CD4+ as compared with control medium (Fig. 5C). The proportion of the pro-T_H17 cytokines IL-22–, IL-17A–, and IL-17F–producing CD4+ T cells was higher after CM Sa-severe stimulation compared with CM Sa-moderate and control medium (Fig. 5C). Concerning MAIT cells, CM Sa-severe stimulation enhanced the production of IL-17A, IL-17F, and IL-22 compared with keratinocyte medium or CM Sa-moderate (Fig. 5C). Of note, the IL-17A, IL-17F, and IL-22 levels globally released by healthy donor PBMCs were also enhanced upon CM Sa-severe compared with keratinocyte medium stimulation (fig. S7).

To further contextualize the inflammatory properties of RDEB *S. aureus* isolates, we also tested the ability of *S. aureus* isolates collected from the skin of patients with atopic dermatitis (AD) and nonpathogenic *Staphylococcus epidermidis* isolates from healthy carriers to stimulate primary keratinocytes. We observed that strains from patients with AD were globally less able to induce proinflammatory cytokines compared with RDEB isolates (fig. S8A). As expected, the *S. epidermidis* strains triggered a distinct response compared with the *S. aureus* strains (fig. S8A) (*24*). Unlike clinical *S. aureus* RDEB strains, neither *S. aureus* strains from patients with AD nor *S. epidermidis* strains from the skin of healthy volunteers were able to significantly increase the frequency of IL-17A+/CD4+ and IL-17F+/CD4+ T cells (fig. S8B). Overall, these results highlight that the inflammatory response triggered by *S. aureus* clinical strains of RDEB appears distinct from that of a reference strain and from that of clinical strains of AD as well as nonpathogenic strains of *S. epidermidis*. These findings are in line with a previous study showing that clinical *S. aureus* AD strains, *S. epidermidis*, and USA300 have distinct abilities to affect the inflammatory response (*25*).

Involvement of Geh lipase in triggering a pro-T_H17 inflammatory response in PBMCs

The molecular mechanisms behind different bacterial behaviors are polyfactorial and may be patient specific. Nevertheless, we attempted to identify some bacterial determinants of disease severity by analyzing shotgun proteomics of the secretomes of our *S. aureus* strains. We compared the secretomes of the group of strains with a high keratinocyte inflammatory response versus the group of strains with a low keratinocyte inflammatory response and identified 159 DEPs (q value < 0.05). Considering only statistically significant proteins with $\log_2$(fold change) $\geq |2|$, we found 48 and 41 DEPs that were up-regulated and down-regulated, respectively, in secretomes from strains with high versus low keratinocyte inflammatory response (selected DEPs with known function and orthologs in the NCTC8325 reference strain are listed in table S3). As expected, proteins predicted to be secreted were found to be enriched by GO enrichment analysis in our clinical strain secretomes (fig. S9). The DEPs were further analyzed with the Search Tool for the Retrieval of Interacting Genes/Proteins database (STRING-db) to identify protein-protein interaction networks and enrichment in functional categories according to KEGG

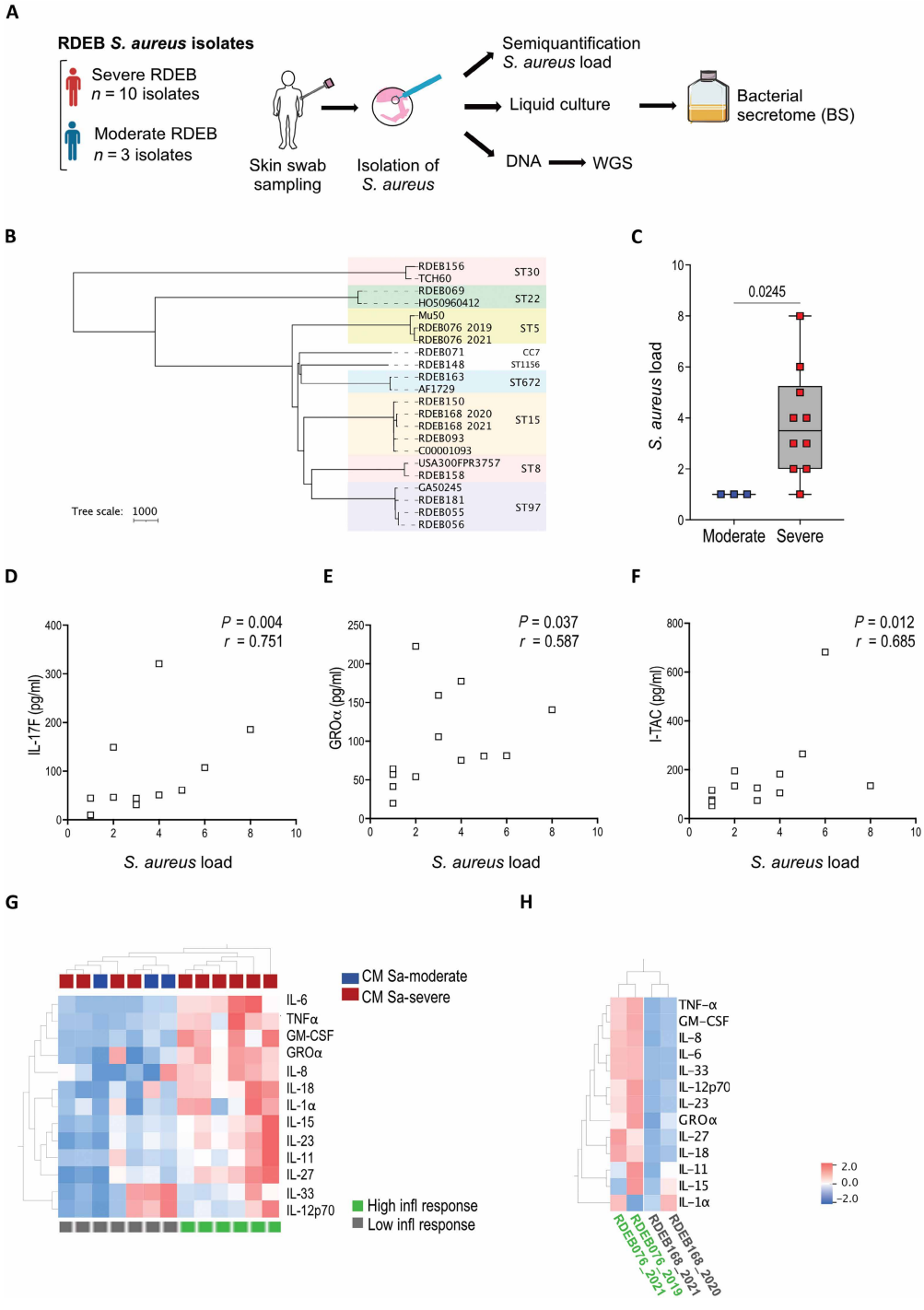

Fig. 4. Clinical *S. aureus* strain profiling and action on keratinocytes. (**A**) Overview of the analyses carried out with *S. aureus* isolates collected from patient skin. WGS, whole-genome sequencing. (**B**) Dendrogram generated by the Pathogenwatch online server on the basis of MLST clustering of the cg assemblies of clinical isolates taken from the skin of 13 patients with RDEB and seven reference genomes from public databases. Branch lengths are proportional to the number of different loci according to the *S. aureus* cgMLST scheme. For two patients with two isolates, the year of isolation is indicated. The ST or clonal complex (CC) of isolates have been indicated where available. Reference strains included are GA50245 (ST97), USA300_FPR3757 (ST8), C00001093 (ST15), Mu50 (ST5), AF1729 (ST672), HO 5096 0412 (ST22), and TCH60 (ST30). (**C**) Box plot showing the median distribution (min to max with all points) of *S. aureus* load according to disease severity (moderate RDEB, $n = 3$ samples; severe RDEB, $n = 10$ samples). (**D** to **F**) Spearman correlation between IL-17F (D), GROα (E), or I-TAC (F) concentration in the plasma of patients with RDEB and *S. aureus* load. (**G**) Heatmap and hierarchical clustering of cytokines released upon primary keratinocyte stimulation by secretomes of *S. aureus* strains collected from the skin of patients with moderate RDEB (CM Sa-moderate) or severe RDEB (SM Sa-severe) revealing two patterns of inflammatory (infl) responses (green, high inflammatory response; gray, low inflammatory response). (**H**) Heatmap showing the ability of *S. aureus* clones collected from the skin of patients with RDEB 1 year (RDEB168_2020) to 2 years (RDEB076_2019) earlier to stimulate primary keratinocytes.

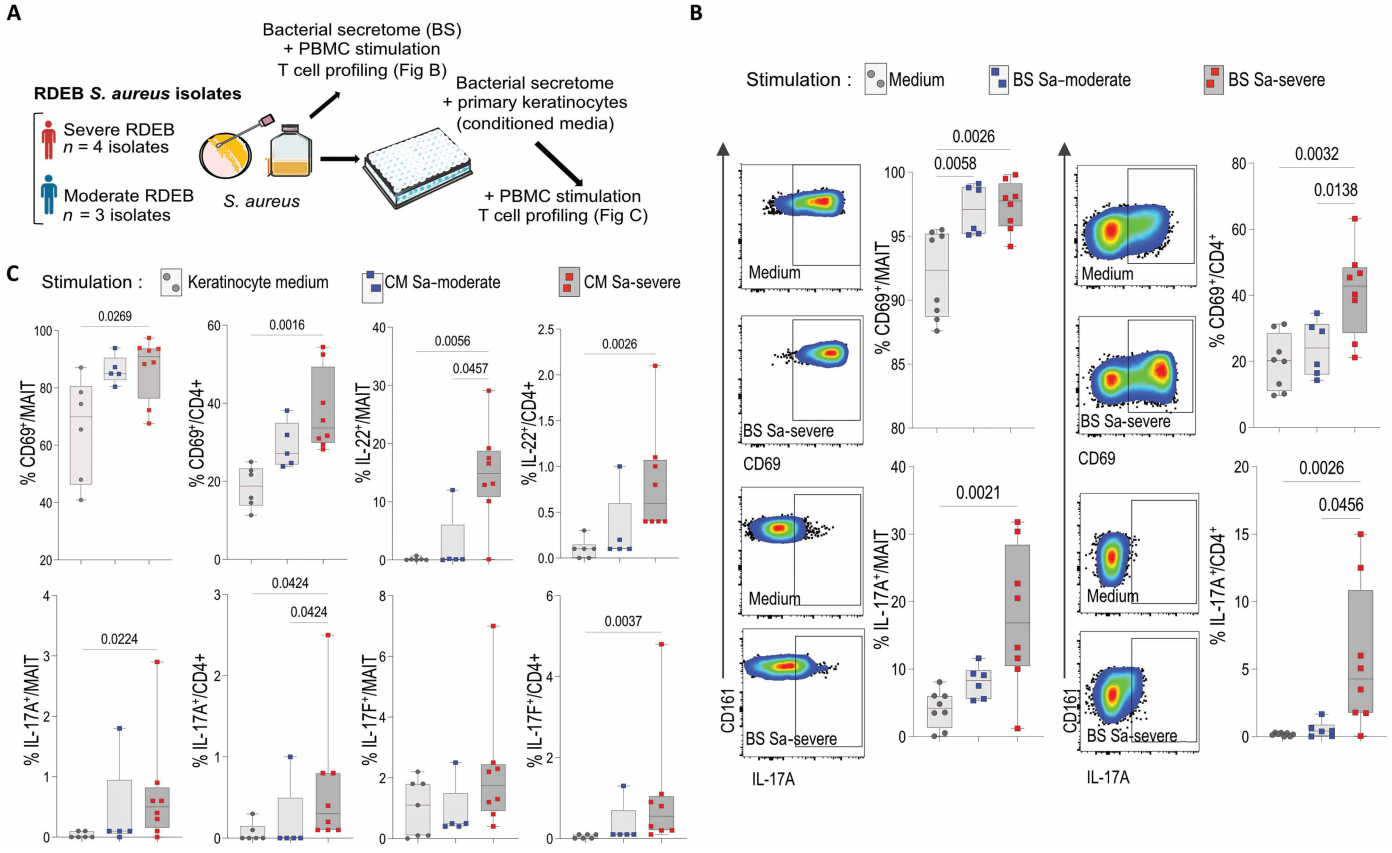

Fig. 5. Impact of clinical strains of *S. aureus* on MAIT and CD4+ T cells. (**A**) Overview of the analyses carried out with secretomes from *S. aureus* strains collected from the patient skin and CM from keratinocytes stimulated with *S. aureus* secretomes. (**B** and **C**) Immune cell profiling of healthy donor PBMCs upon 24-hour stimulation by BS (BS Sa-moderate, $n = 3$; BS Sa-severe, $n = 4$) (B) or CM from primary keratinocytes stimulated by *S. aureus* strains collected from the patient skin (CM Sa-moderate, $n = 3$; CM Sa-severe, $n = 4$) (C). Data are indicated as medians (min to max with all points). Two independent experiments were performed. Statistical differences were determined by the Kruskal-Wallis test with Benjamini-Hochberg corrections. Significant q values ($q < 0.05$) are indicated.

keywords (*26*). We found an enrichment in virulence-associated proteins [KEGG keyword KW-0843—"virulence"; strength = 0.83, false discovery rate (FDR) = 0.0498] and an enrichment in proteases (KEGG keyword KW-0645—"protease"; strength = 1.09, FDR = 0.0258) in up-regulated (Fig. 6A) and down-regulated (Fig. 6B) DEPs, respectively, in the secretomes of strains with a high keratinocyte inflammatory response.

As proof of concept, we focused further on the secreted lipase Geh, a known immunomodulatory protein, found in the down-regulated DEPs in *S. aureus* isolates with higher inflammatory properties (Fig. 6B). Geh is known to inhibit activation of innate immune cells, and in turn, a *geh* mutant has been shown to increase cytokine production in primary murine bone marrow–derived macrophages (*27*, *28*). To evaluate the potential contribution of this secreted lipase, we tested a *geh* mutant from the Nebraska Transposon Mutant Library (NTML) along with its complemented derivative. We found that IL-23, IL-12p70, IL-27, and IL-11 were increased in primary keratinocytes stimulated by the *geh* mutant compared with the reference strain or the complemented mutant (fig. S10). This indicates that *geh* can modify cytokines released by keratinocytes in line with the expected immunomodulatory effect of Geh.

IL-23 plays a central role in the expansion and function of proinflammatory T_H17 cells (*29*). A recent study has shown that IL-23 and IL-12p70 increase the frequency of IL-17–producing MAIT cells (*29*). Because the NTML *geh* mutant increased secretion of these cytokines and *geh* complementation restored normal expression (fig. S10), we reasoned that expressing wild-type *geh* in clinical *S. aureus* strains from patients with severe RDEB could decrease the concentrations of IL-23 and IL-12p70 released by keratinocytes. Therefore, we expressed wild-type *geh* in three clinical *S. aureus* strains isolated from patients with severe RDEB (Sa-RDEB *geh* comp). Primary keratinocytes secreted lower amounts of IL-12p70 and IL-23 when stimulated with Sa-RDEB *geh* comp compared with the original strains, with significant reduction observed in three ($P = 0.050$) and two ($P = 0.050$) strains, respectively (Fig. 6C). In addition, CM from Sa-RDEB *geh* comp significantly decreased the frequency of CD69+/MAIT (two strains $P = 0.079$), IL-17F+/MAIT (two strains $P = 0.0317$ and 0.0079), IL-22+/MAIT (one strain $P = 0.0317$), CD69+/CD4+ (one strain $P = 0.0476$), IL-17A+/CD4+ (two strains $P = 0.0079$ and 0.0278), and IL-22+/CD4+ (one strain $P = 0.0476$) cells (Fig. 6, D to F). The fact that this single-gene complementation partially counteracted the inflammatory response triggered by clinical RDEB strains highlights the polyfactorial nature of the RDEB immune response, with Geh being one of the bacterial contributing factors.

A recent study identified keratinocyte-derived lactate as a driver of the skin IL-17 response (*30*). We thus investigated lactate released

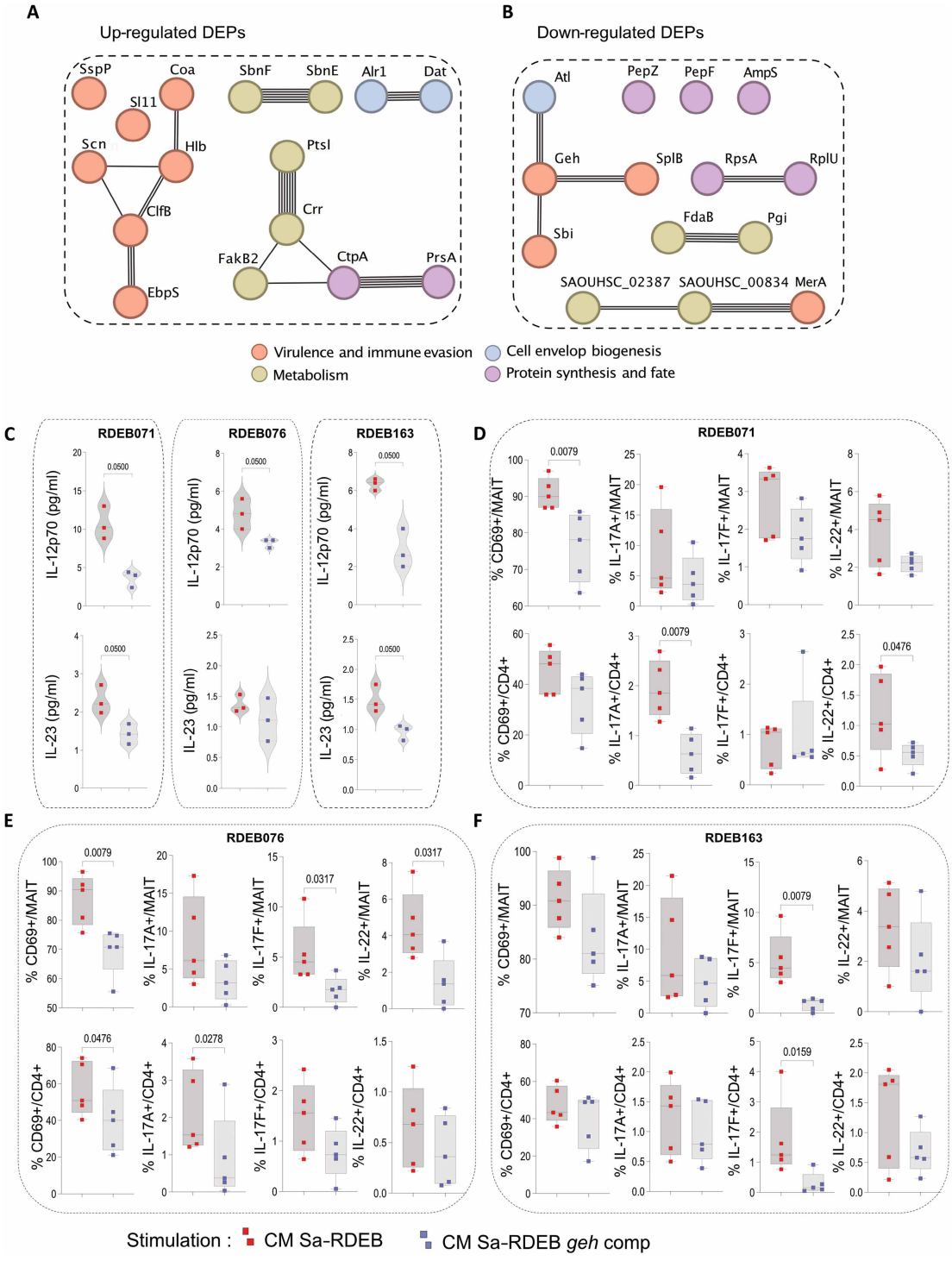

Fig. 6. Clinical *S. aureus* strain secretome profiling and cytokine production. (**A** and **B**) STRING protein-protein interaction networks (PPIs) identified among DEPs in *S. aureus* secretomes triggering a strong keratinocyte inflammatory response. (A) PPIs among up-regulated DEPs. (B) PPIs among down-regulated DEPs including the secreted lipase Geh. Functional categories are indicated with a color code and detailed in table S3. Line thickness between protein nodes indicates the STRING-db confidence score of the interaction between the connected proteins, with higher confidence scores represented by thicker lines. (**C**) Cytokines released upon primary keratinocyte stimulation by secretomes of clinical *S. aureus* strains from the patients RDEB071, RDEB076, and RDEB163 (red square) and wild-type *geh*–complemented strains (blue square). (**D** to **F**) Profiling of healthy donor PBMCs upon stimulation by CM from primary keratinocytes stimulated by secretomes of clinical *S. aureus* strains from the patients RDEB071, RDEB076, and RDEB163 (red square) and wild-type *geh*–complemented strains (blue square). Data are indicated as medians (min to max with all points). PBMCs from five donors were tested. Statistical differences were determined by the Kruskal-Wallis test. Significant *P* values ($P < 0.05$) are indicated.

by *S. aureus*–stimulated keratinocytes. We found that keratinocytes stimulated by *S. aureus* release lactate into the medium (fig. S11). Of note, the quantity of lactate released varied among different *S. aureus* strains tested. However, our analysis revealed no substantial correlation between the severity of the disease and the amount of lactate released (fig. S11). These findings suggest that keratinocyte-derived lactate could potentially contribute to the IL-17 response of the patient, further supporting the multifactorial nature of the IL-17 response induced by *S. aureus* clinical isolates.

DISCUSSION

We analyzed a cohort of pediatric patients with a rare genetic dermatosis as a model disease to establish their immune characteristics and their association with *S. aureus* skin dysbiosis. We demonstrated that patients with the most severe form of the disease exhibit a skewed T_H17 immune response. Furthermore, our results indicate that *S. aureus* clones from the skin of patients with severe RDEB can preferentially induce IL-17A production by MAIT and CD4+ T cells. The mechanisms involved are polyfactorial; however, our results indicate that Geh lipase may play a role.

Elevated quantities of circulating cytokines have already been reported and correlated with disease severity in patients with EB (*31*–*33*). Besides, transcriptomic analysis of RDEB versus normal skin revealed increased expression of several genes involved in immune system activation (*34*). All of these data led us to consider RDEB as an immunopathological disease, for which the complex intertwining between skin inflammation and immune response needs to be better understood. Our results highlighted that the frequency of IL-17A–producing CD4+ and MAIT cells was higher in patients with severe RDEB than in controls. Consistent with these findings, we found that patients with severe RDEB also had higher plasma concentrations of IL-17A, IL-17F, and IL-22, the major cytokines associated with the T_H17 immune response (*35*–*37*). IL-17A is a proinflammatory cytokine that acts primarily on nonhematopoietic cells to induce acute innate immune defenses (*35*–*37*). A link between IL-17A and chronic inflammatory skin diseases, including psoriasis, AD, Netherton syndrome, and systemic sclerosis, has already been reported (*38*, *39*). This cytokine can be produced not only by a subset of conventional CD4+ T cells, commonly known as T_H17 cells, but also by other cell populations, notably MAIT cells. MAIT cells are one of the main T cell populations present in the human skin. Experimental models have demonstrated that MAIT cells are involved in wound healing through their ability to produce IL-17A or amphiregulin (*3*, *10*). However, the contribution of MAIT cells to human skin inflammation, including that observed in patients with severe RDEB, remains to be determined. In essence, our results revealed a possible unexpected involvement of IL-17A–producing MAIT cells in the inflammatory response observed in patients with severe RDEB.

COL7A1 gene mutations in patients with RDEB result in extreme skin fragility, tissue damage, and remodeling. Higher frequencies of T_H17 and MAIT17 cells and plasma IL-17A and IL-17F are present in patients with RDEB. IL-17 promotes tissue repair and protective immunity against pathogens, but if its production is excessive, it can also contribute to inflammatory disease and fibrosis (*36*, *40*). Actually, IL-17 can induce the production of matrix metalloproteinases (MMPs) and ECM proteins involved in fibrosis (*41*–*43*). Overall, these results indicate that the elevated IL-17 quantities observed in RDEB may contribute to skin damage. Whereas previous studies have focused on proteomic profiling of skin biopsies or primary fibroblasts collected from patients with RDEB (*44*, *45*), in the present study, we used state-of-the-art unbiased direct proteomics of neat plasma, allowing analysis of more than 800 proteins. Proteomic profiling distinguished severe RDEB, moderate RDEB, and control groups, with the moderate RDEB group being between the severe RDEB and control groups. Overall, the proteins and pathways deregulated in severe RDEB indicate a strong inflammatory response and ECM dysfunction. The most DEPs down-regulated in patients with RDEB belonged to the collagen-containing ECM category. This type of down-regulation has already been reported in major inflammatory conditions. Plasma proteomic analysis of patients with COVID-19 identified ECM degradation, exemplified by the up-regulation of MMP2, that was associated with severity of infection (*46*). Both plasmatic MMP2 and MMP9 were augmented in the plasma of patients with RDEB compared with controls. These results are in line with our previous report, which showed enhanced skin expression of metalloproteinases in clinical RDEB (*47*). Together, they indicate that MMPs could be involved in the epidermal detachment observed in RDEB.

We hypothesized that chronic infection of RDEB wounds by *S. aureus* may contribute to the severity of RDEB disease. Furthermore, we demonstrated the ability of *S. aureus* strains from patients with severe RDEB to polarize the immune response toward a T_H17 profile in vitro, which could account for the T_H17 response observed in patients. For two patients, we showed the long-term persistence of the same clone with similar proinflammatory properties. Hence, *S. aureus* long-term colonization by selected clones could be a trigger to redirect immune response toward the T_H17 pathway.

The importance of the T_H17 responses for host defense against *S. aureus* infections is highlighted by the fact that patients with STAT3 mutations (hyper-IgE syndrome) that are associated with T_H17 defects are known to exhibit severe and recurrent *S. aureus* skin infections (*48*). Several studies in mice or humans have also shown the importance of IL-17 production in providing immunity against *S. aureus* infections (*48*–*52*). Furthermore, increased concentrations of IL-17A were reported in the sera of patients with *S. aureus* chronic suppurative dermatitis or chronic lung infections (*53*). Known bacterial determinants of IL-17 production include alpha-toxin, SEB superantigen (*54*), peptidoglycan shedding (*55*), and phenol-soluble modulins (*52*, *56*) by acting directly or indirectly on CD4+ T cells. MAIT cells can be stimulated not only by *S. aureus* antigens but also by cytokines such as IL-1, IL-12, IL-15, IL-23, and IL-33, which were present in CM obtained by stimulating primary keratinocytes with *S. aureus* strains from patients with severe RDEB. In response to these TCR-dependent or TCR-independent stimulators, MAIT cells can produce IFN-γ or IL-17A (*57*–*60*).

The strains associated with RDEB belong to common clones circulating in France (including ST30, ST22, ST5, ST15, and ST8 also present in the French cohort of children with cystic fibrosis) (*61*, *62*). An unresolved question is how the skin of a patient with severe RDEB can affect the virulence program of *S. aureus* differently compared with patients with moderate disease. The skin environment of RDEB imposes stress conditions on *S. aureus* strains (local inflammation, local treatments, and antibiotics), which can have a direct impact on the transcription of virulence factors and act as selective pressures favoring the emergence of genetic variants accumulating adaptive mutations that modify their virulence profile. These

selective pressures are strongest in severe forms of the disease. For instance, exposure to antibiotics and disinfectants has been shown to profoundly alter the transcriptional program of *S. aureus* (*63*–*65*). In particular, cell wall–damaging antibiotics such as beta-lactams trigger a global stress response with increased production of staphylococcal exotoxins, including the key virulence factors alpha-toxin and Panton-Valentine leukocidin (PVL). In addition, staphylococcal virulence regulators are likely to contribute to different behaviors between *S. aureus* strains infecting patients with severe or moderate disease (*66*, *67*). However, for many *S. aureus* virulence regulators, we still lack knowledge of the microenvironmental signals sensed at infected sites.

We acknowledge that our study has certain limitations. A first limitation lies in the lack of evaluation of tissues other than blood, in particular the skin. It has been reported that proinflammatory cytokines dominate the blister fluids of patients with EB (*68*). These inflammatory cytokines could affect the local cellular immune response and the selection of *S. aureus* clones, which would be interesting to study. A second limitation is the limited number of patients. For the purposes of our study, it was important to obtain *S. aureus* and blood samples from each patient at the same time. This constraint, combined with the fact that RDEB is a rare disease, contributed to limiting the number of patients analyzed. Furthermore, it is not possible to deduce, on the basis of these results, how or when wounds may have been preferentially colonized by a given *S. aureus* clone. Although we observed the persistence of two *S. aureus* clones for at least a year, it would be important to follow longitudinally the evolution of the strains in parallel with the evolution of the immune response. Future work will be needed to understand the drivers of selection of *S. aureus* persistent clones, the molecular mechanisms of their inflammatory behavior including their capacity to induce a pro-T_H17 immune response, and the long-term consequences of patient immune system stimulation by persistent clones (for example, inflammatory and fibrotic responses and oncogenesis) in the context of chronic skin infections.

Knowing that the use of monoclonal antibodies (mAbs) against IL-17A, such as secukinumab, ixekizumab, and brodalumab, and against both IL-17A and IL-17F (bimekizumab) is effective for a number of patients with chronic skin diseases (*69*–*72*), our results could provide a rationale to test this type of targeted therapy in patients with severe RDEB. Furthermore, untargeted approaches used in this study could pave the way for discovery of future noninvasive biomarkers to assess treatment efficacy.

MATERIALS AND METHODS

Study design

The goal of this study was to take advantage of a unique cohort of patients with chronic wounds associated with *S. aureus* skin dysbiosis to better understand the relationship between patient strains and the immune response elicited. For this, we used proteomic, immunological profiling, and in vitro assays to perform an in-depth immune analysis of severe and moderate clinical RDEB. On the same day, we also obtained skin samples from 13 patients with RDEB for selective detection, semiquantification, whole-genome sequencing, and analysis of *S. aureus*. In vitro assays using secretomes from *S. aureus* strains collected from the patient skin and CM from primary keratinocytes stimulated with these clinical strains were used to stimulate circulant CD4+ and MAIT cells. Activation state and cytokine production by these cells in response to the stimulations were analyzed. Each in vitro experiment was performed as independently as possible. As such, experiments were repeated on different days with cells from distinct donors and different *S. aureus* secretomes and CM stocks.

Ethics statement

All experiments were performed in accordance with the guidelines and regulations described by the Declaration of Helsinki and the Huriet-Serusclat law on human research ethics. The study was registered with the AP-HP5 Department of Data Protection (reference: no. 2023 0428174811 and NCT03776474) for the control group (without skin diseases or allergy). Patients' parents or guardians were informed about the study's objectives and procedures. The clinical evaluation was performed by two expert clinicians for patients with EB (CB and NB) at the French national center for patients with genodermatoses MAGEC. A validated specific EB score of severity, EBDASI (*73*), was used to score the clinical severity of the patients during the study period (April to December 2021). EBDASI is a partially validated EB-specific instrument that assesses disease activity and damage at 12 cutaneous sites in addition to the scalp, mucous membranes, nails, and other epithelialized surfaces. Total activity (of 276) and damage (of 230) are combined to give an overall score of 506. Total EBDASI score ranges of 0 to 106 and 107 to 506 corresponded to moderate and severe involvement, respectively. Patient characteristics are described in Table 1.

Flow cytometry and T cell culture

Freshly isolated PBMCs were obtained using Ficoll-Paque density centrifugation (1.077 g/ml; PAA Laboratories GmbH). Cells were then resuspended and washed in fluorescence-activated cell sorting (FACS) buffer [2% (w/v) bovine serum albumin and 0.1% NaN_3 sodium azide in phosphate-buffered saline]. For detection of live cells, fixable viability dye eFluor 506 (eBioscience) was used. Cells were stained for 30 min at 4°C for surface staining. For intracellular cytokine analysis allowing the identification of IL-4–, IL-13–, IL-17A–, IL-17F–, IL-22–, TNFα-, and IFN-γ–producing T cells (gating strategy in figs. S2 and S3), PBMCs were cultured for 5 hours with PMA (25 ng/ml) and 1 μM ionomycin in the presence of brefeldin A (10 ng/ml) (all from Sigma-Aldrich). The fluorochrome-conjugated antibodies used are presented in table S4. MR1-5-OP-RU-PE tetramers and the respective controls were kindly provided by the NIH Tetramer Core Facility. Events were acquired on a FACS LSR Fortessa (BD Biosciences) and analyzed using FlowJo software v10.8.1 (Becton, Dickinson and Company).

Bacterial culture

Skin samples were collected from patients following the routine procedure of the dermatology department as follows: After gently cleaning the lesion with saline solution, an ESwab (Copan) was twirled on the lesion area. The ESwab system, which includes a nylon-flocked swab for sample collection and a transport tube containing 1 ml of liquid Amies transport medium, was sent to the Necker Hospital microbiology laboratory for processing within 2 hours of collection. For routine semiquantitative determination of *S. aureus* load, a 10-μl aliquot of ESwab liquid medium was inoculated onto CHROMID *S. aureus* Elite agar selective medium (bioMérieux) and streaked in quadrants. Positive cultures were further characterized using MALDI Biotyper (Bruker Daltonics) identification. On the basis of visual

inspection of the plate after 48 hours of growth at 35°C, the *S. aureus* load of each sampled site was classified as follows: 0, no growth; 1, growth in the first quadrant; 2, growth in the second quadrant; 3, growth in the third quadrant; and 4, growth in the fourth quadrant. The final *S. aureus* load, ranging from 0 to 8, corresponded to the sum of the two body sites sampled by the physician according to the patient's wounds.

Primary keratinocyte culture and CM preparation

Normal primary human epidermal keratinocytes (HPEKps, CELLnTEC) were propagated in serum-free CnT-07 medium as per the manufacturer's instructions (CELLnTEC). HPEKps were seeded in 96-well microtiter plates (coated with collagen) in CnT07 and incubated for 96 hours (37°C, 5% CO_2) with renewal of the medium at 48 hours. At 96 hours, CnT07 medium was removed and either RPMI–fetal calf serum (FCS) (to assess basal cytokine concentrations) or 1:2 dilution of standardized culture secretomes was added. After 4 hours of stimulation (at 37°C, 5% CO_2), CM was collected and stored at −80°C until use.

PBMC profiling upon stimulation by BS or CM

PBMCs from four distinct healthy donors [Établissement Français du Sang (EFS)] were cultured at a density of 2.5×10^6 cells/ml in RPMI 1640 medium supplemented with antibiotics, 10% FCS, and 200 mM glutamine (GIBCO, Fisher Scientific SAS) and IL-2 (5 ng/ml, R&D Systems). Cells were stimulated for 24 hours with culture secretomes, medium, or conditioned HPEKp medium at 1/10. Brefeldin A (10 μg/ml; Sigma-Aldrich) was added for the last 4 hours. Cells were collected and immunostained to detect cytokine-producing cells as described in the "Flow cytometry and T cell culture" section. Selected *S. aureus* and *S. epidermidis* isolates were used to obtain secretomes and conditioned HPEKp medium to stimulate PBMCs. Two distinct experiments were performed. Results were pooled per experiment according to the stimulation used. PBMCs cultured with medium and not stained with anti-CD69 and anti–IL-17A mAbs were used as FMO (fluorescence minus one) controls (fig. S6B).

S. aureus whole-genome sequencing and analysis

Genomic DNA of *S. aureus* strains was extracted using the DNeasy Blood and Tissue Kit with lysostaphin (10 μg/ml) to facilitate bacterial cell wall lysis. Genomic libraries were prepared using a Nextera XT kit, multiplexed, and sequenced on an Illumina MiniSeq instrument (2 × 150 paired-end sequencing). The raw reads were de novo assembled using Unicycler (*74*) and annotated using PROKKA (*75*). ST assignment was performed on the Pathogenwatch online server developed by the Center for Genomic Pathogen Surveillance (https://pathogen.watch) and relies on MLST (multilocus sequence typing) schemes provided by PubMLST. A dendrogram performed by Pathogenwatch has been inferred on the basis of core genome (cg) MLST clustering, by calculating distances between each assembly. The distance represents the number of different loci in the Pathogenwatch *S. aureus* cgMLST scheme. The sequences reported here are available at NCBI's BioProject database under accession number PRJNA961692.

Statistical analysis

Differences between the groups were assessed with a two-sided Kruskal-Wallis test. *P* values were adjusted for multiple hypotheses using the Benjamini-Hochberg procedure to produce FDRs and were considered statistically significant when *q* values were less than 0.05. Correlations between two parameters were assessed using Spearman's ranking correlation. GraphPad Prism 9.0 software was used for statistical tests. PLS-DA (Fig. 2A) was performed using R (version 1.2.5033), and heatmaps were performed using Qlucore Omics Explorer (version 3.7-24). Proteomics analysis was performed using R language (www.R-project.org) and Bioconductor Project packages (www.bioconductor.org).

Supplementary Materials

The PDF file includes:
Materials and Methods
Figs. S1 to S11
Tables S1 to S4
References (*76–82*)

Other Supplementary Material for this manuscript includes the following:
Data files S1 to S3
MDAR Reproducibility Checklist

REFERENCES AND NOTES

1. D. I. Godfrey, H. F. Koay, J. McCluskey, N. A. Gherardin, The biology and functional importance of MAIT cells. *Nat. Immunol.* **20**, 1110–1128 (2019).
2. I. Nel, L. Bertrand, A. Toubal, A. Lehuen, MAIT cells, guardians of skin and mucosa? *Mucosal Immunol.* **14**, 803–814 (2021).
3. M. G. Constantinides, V. M. Link, S. Tamoutounour, A. C. Wong, P. J. Perez-Chaparro, S. J. Han, Y. E. Chen, K. Li, S. Farhat, A. Weckel, S. R. Krishnamurthy, I. Vujkovic-Cvijin, J. L. Linehan, N. Bouladoux, E. D. Merrill, S. Roy, D. J. Cua, E. J. Adams, A. Bhandoola, T. C. Scharschmidt, J. Aube, M. A. Fischbach, Y. Belkaid, MAIT cells are imprinted by the microbiota in early life and promote tissue repair. *Science* **366**, eaax6624 (2019).
4. E. Treiner, L. Duban, S. Bahram, M. Radosavljevic, V. Wanner, F. Tilloy, P. Affaticati, S. Gilfillan, O. Lantz, Selection of evolutionarily conserved mucosal-associated invariant T cells by MR1. *Nature* **422**, 164–169 (2003).
5. L. Kjer-Nielsen, O. Patel, A. J. Corbett, J. Le Nours, B. Meehan, L. Liu, M. Bhati, Z. Chen, L. Kostenko, R. Reantragoon, N. A. Williamson, A. W. Purcell, N. L. Dudek, M. J. McConville, R. A. O'Hair, G. N. Khairallah, D. I. Godfrey, D. P. Fairlie, J. Rossjohn, J. McCluskey, MR1 presents microbial vitamin B metabolites to MAIT cells. *Nature* **491**, 717–723 (2012).
6. J. Li, R. Reantragoon, L. Kostenko, A. J. Corbett, G. Varigos, F. R. Carbone, The frequency of mucosal-associated invariant T cells is selectively increased in dermatitis herpetiformis. *Australas. J. Dermatol.* **58**, 200–204 (2017).
7. G. Lezmi, R. Abou-Taam, N. Garcelon, C. Dietrich, F. Machavoine, C. Delacourt, K. Adel-Patient, M. Leite-de-Moraes, Evidence for a MAIT-17-high phenotype in children with severe asthma. *J. Allergy Clin. Immunol.* **144**, 1714–1716.e6 (2019).
8. J. R. Victor, G. Lezmi, M. Leite-de-Moraes, New insights into asthma inflammation: Focus on iNKT, MAIT, and γδT cells. *Clin. Rev. Allergy Immunol.* **59**, 371–381 (2020).
9. K. T. Maleki, J. Tauriainen, M. García, P. F. Kerkman, W. Christ, J. Dias, J. W. Byström, E. Leeansyah, M. N. Forsell, H.-G. Ljunggren, C. Ahlm, N. K. Björkström, J. K. Sandberg, J. Klingström, MAIT cell activation is associated with disease severity markers in acute hantavirus infection. *Cell Rep. Med.* **2**, 100220 (2021).
10. A. du Halgouet, A. Darbois, M. Alkobtawi, M. Mestdagh, A. Alphonse, V. Premel, T. Yvorra, L. Colombeau, R. Rodriguez, D. Zaiss, Y. El Morr, H. Bugaut, F. Legoux, L. Perrin, S. Aractingi, R. Golub, O. Lantz, M. Salou, Role of MR1-driven signals and amphiregulin on the recruitment and repair function of MAIT cells during skin wound healing. *Immunity* **56**, 78–92.e6 (2023).
11. J.-D. Fine, Epidemiology of inherited epidermolysis bullosa based on incidence and prevalence estimates from the National Epidermolysis Bullosa Registry. *JAMA Dermatol.* **152**, 1231–1238 (2016).
12. R. Varki, S. Sadowski, J. Uitto, E. Pfendner, Epidermolysis bullosa. II. Type VII collagen mutations and phenotype-genotype correlations in the dystrophic subtypes. *J. Med. Genet.* **44**, 181–192 (2007).
13. C. Has, J. W. Bauer, C. Bodemer, M. C. Bolling, L. Bruckner-Tuderman, A. Diem, J. D. Fine, A. Heagerty, A. Hovnanian, M. P. Marinkovich, A. E. Martinez, J. A. McGrath, C. Moss, D. F. Murrell, F. Palisson, A. Schwieger-Briel, E. Sprecher, K. Tamai, J. Uitto, D. T. Woodley, G. Zambruno, J. E. Mellerio, Consensus reclassification of inherited epidermolysis bullosa and other disorders with skin fragility. *Br. J. Dermatol.* **183**, 614–627 (2020).
14. A. Hovnanian, A. Rochat, C. Bodemer, E. Petit, C. A. Rivers, C. Prost, S. Fraitag, A. M. Christiano, J. Uitto, M. Lathrop, Y. Barrandon, Y. de Prost, Characterization of 18 new mutations in COL7A1 in recessive dystrophic epidermolysis bullosa provides evidence for

distinct molecular mechanisms underlying defective anchoring fibril formation. *Am. J. Hum. Genet.* **61**, 599–610 (1997).
15. A. Nyström, L. Bruckner-Tuderman, D. Kiritsi, Dystrophic epidermolysis bullosa: Secondary disease mechanisms and disease modifiers. *Front. Genet.* **12**, 737272 (2021).
16. A. Nystrom, O. Bornert, T. Kuhl, C. Gretzmeier, K. Thriene, J. Dengjel, A. Pfister-Wartha, D. Kiritsi, L. Bruckner-Tuderman, Impaired lymphoid extracellular matrix impedes antibacterial immunity in epidermolysis bullosa. *Proc. Natl. Acad. Sci. U.S.A.* **115**, E705–E714 (2018).
17. J. Bar, O. Sarig, M. Lotan-Pompan, B. Dassa, M. Miodovnik, A. Weinberger, E. Sprecher, E. Segal, L. Samuelov, Evidence for cutaneous dysbiosis in dystrophic epidermolysis bullosa. *Clin. Exp. Dermatol.* **46**, 1223–1229 (2021).
18. I. Fuentes, C. Guttmann-Gruber, A. S. L. Tay, J. Pinon Hofbauer, S. Denil, J. Reichelt, F. Palisson, J. E. A. Common, A. P. South, Reduced microbial diversity is a feature of recessive dystrophic epidermolysis bullosa-involved skin and wounds. *J. Invest. Dermatol.* **138**, 2492–2495 (2018).
19. A. Reimer-Taschenbrecker, A. Kunstner, M. Hirose, S. Hubner, S. Gewert, S. Ibrahim, H. Busch, C. Has, Predominance of *Staphylococcus* correlates with wound burden and disease activity in dystrophic epidermolysis bullosa: A prospective case-control study. *J. Invest. Dermatol.* **142**, 2117–2127.e8 (2022).
20. S. van den Berg, D. G. A. M. Koedijk, J. W. Back, J. Neef, A. Dreisbach, J. M. van Dijl, I. A. Bakker-Woudenberg, G. Buist, Active immunization with an octa-valent *Staphylococcus aureus* antigen mixture in models of *S. aureus* bacteremia and skin infection in mice. *PLOS ONE* **10**, e0116847 (2015).
21. J. M. Wozniak, R. H. Mills, J. Olson, J. R. Caldera, G. D. Sepich-Poore, M. Carrillo-Terrazas, C. M. Tsai, F. Vargas, R. Knight, P. C. Dorrestein, G. Y. Liu, V. Nizet, G. Sakoulas, W. Rose, D. J. Gonzalez, Mortality risk profiling of *Staphylococcus aureus* bacteremia by multi-omic serum analysis reveals early predictive and pathogenic signatures. *Cell* **182**, 1311–1327. e14 (2020).
22. W. Chen, X. Qiang, Y. Wang, S. Zhu, J. Li, A. Babaev, H. Yang, J. Gong, L. Becker, P. Wang, K. J. Tracey, H. Wang, Identification of tetranectin-targeting monoclonal antibodies to treat potentially lethal sepsis. *Sci. Transl. Med.* **12**, eaaz3833 (2020).
23. M. M. van der Kooi-Pol, Y. K. Veenstra-Kyuchukova, J. C. Duipmans, G. N. Pluister, L. M. Schouls, A. J. de Neeling, H. Grundmann, M. F. Jonkman, J. M. van Dijl, High genetic diversity of *Staphylococcus aureus* strains colonizing patients with epidermolysis bullosa. *Exp. Dermatol.* **21**, 463–466 (2012).
24. Ó. Burke, M. S. Zeden, J. P. O'Gara, The pathogenicity and virulence of the opportunistic pathogen *Staphylococcus epidermidis*. *Virulence* **15**, 2359483 (2024).
25. A. L. Byrd, C. Deming, S. K. B. Cassidy, O. J. Harrison, W. I. Ng, S. Conlan, N. C. S. Program, Y. Belkaid, J. A. Segre, H. H. Kong, *Staphylococcus aureus* and *Staphylococcus epidermidis* strain diversity underlying pediatric atopic dermatitis. *Sci. Transl. Med.* **9**, eaal4651 (2017).
26. D. Szklarczyk, R. Kirsch, M. Koutrouli, K. Nastou, F. Mehryary, R. Hachilif, A. L. Gable, T. Fang, N. T. Doncheva, S. Pyysalo, P. Bork, L. J. Jensen, C. von Mering, The STRING database in 2023: Protein-protein association networks and functional enrichment analyses for any sequenced genome of interest. *Nucleic Acids Res.* **51**, D638–D646 (2023).
27. X. Chen, F. Alonzo III, Bacterial lipolysis of immune-activating ligands promotes evasion of innate defenses. *Proc. Natl. Acad. Sci. U.S.A.* **116**, 3764–3773 (2019).
28. X. Tan, M. Coureuil, A. Charbit, A. Jamet, Multitasking actors of *Staphylococcus aureus* metabolism and virulence. *Trends Microbiol.* **28**, 6–9 (2020).
29. C. de Jesús-Gil, E. Ruiz-Romeu, M. Ferran, M. Sagristà, A. Chiriac, P. García, A. Celada, R. M. Pujol, L. F. Santamaria-Babí, IL-15 and IL-23 synergize to trigger Th17 response by CLA^+ T cells in psoriasis. *Exp. Dermatol.* **29**, 630–638 (2020).
30. I. Subudhi, P. Konieczny, A. Prystupa, R. L. Castillo, E. Sze-Tu, Y. Xing, D. Rosenblum, I. Reznikov, I. Sidhu, C. Loomis, C. P. Lu, N. Anandasabapathy, M. Suárez-Fariñas, J. E. Gudjonsson, A. Tsirigos, J. U. Scher, S. Naik, Metabolic coordination between skin epithelium and type 17 immunity sustains chronic skin inflammation. *Immunity* **57**, 1665–1680.e7 (2024).
31. M. Tampoia, L. Abbracciavento, M. Morrone, R. Fumarulo, IL-6/IL-10 ratio as a prognostic and predictive marker of the severity of inherited epidermolysis bullosa. *Iran. J. Immunol.* **14**, 340–349 (2017).
32. G. Annicchiarico, M. G. Morgese, S. Esposito, G. Lopalco, M. Lattarulo, M. Tampoia, D. Bonamonte, L. Brunetti, A. Vitale, G. Lapadula, L. Cantarini, F. Iannone, Proinflammatory cytokines and antiskin autoantibodies in patients with inherited epidermolysis bullosa. *Medicine* **94**, e1528 (2015).
33. S. Esposito, S. Guez, A. Orenti, G. Tadini, G. Scuvera, L. Corti, A. Scala, E. Biganzoli, E. Berti, N. Principi, Autoimmunity and cytokine imbalance in inherited epidermolysis bullosa. *Int. J. Mol. Sci.* **17**, 1625 (2016).
34. J. S. Breitenbach, M. Rinnerthaler, A. Trost, M. Weber, A. Klausegger, C. Gruber, D. Bruckner, H. A. Reitsamer, J. W. Bauer, M. Breitenbach, Transcriptome and ultrastructural changes in dystrophic Epidermolysis bullosa resemble skin aging. *Aging* **7**, 389–411 (2015).
35. A. Schnell, D. R. Littman, V. K. Kuchroo, T_H17 cell heterogeneity and its role in tissue inflammation. *Nat. Immunol.* **24**, 19–29 (2023).
36. J. Li, J.-L. Casanova, A. Puel, Mucocutaneous IL-17 immunity in mice and humans: Host defense vs. excessive inflammation. *Mucosal Immunol.* **11**, 581–589 (2018).
37. S. L. Gaffen, Structure and signalling in the IL-17 receptor family. *Nat. Rev. Immunol.* **9**, 556–567 (2009).
38. T. Czarnowicki, H. He, A. Leonard, K. Malik, S. Magidi, S. Rangel, K. Patel, K. Ramsey, M. Murphrey, T. Song, Y. Estrada, H. C. Wen, J. G. Krueger, E. Guttman-Yassky, A. S. Paller, The major orphan forms of ichthyosis are characterized by systemic T-cell activation and Th-17/Tc-17/Th-22/Tc-22 polarization in blood. *J. Invest. Dermatol.* **138**, 2157–2167 (2018).
39. C. W. Lynde, Y. Poulin, R. Vender, M. Bourcier, S. Khalil, Interleukin 17A: Toward a new understanding of psoriasis pathogenesis. *J. Am. Acad. Dermatol.* **71**, 141–150 (2014).
40. S. Majumder, M. J. McGeachy, IL-17 in the pathogenesis of disease: Good intentions gone awry. *Annu. Rev. Immunol.* **39**, 537–556 (2021).
41. D. M. Cortez, M. D. Feldman, S. Mummidi, A. J. Valente, B. Steffensen, M. Vincenti, J. L. Barnes, B. Chandrasekar, IL-17 stimulates MMP-1 expression in primary human cardiac fibroblasts via p38 MAPK- and ERK1/2-dependent C/EBP-β, NF-κB, and AP-1 activation. *Am. J. Physiol. Heart Circ. Physiol.* **293**, H3356–H3365 (2007).
42. J. Zhang, D. Wang, L. Wang, S. Wang, A. C. Roden, H. Zhao, X. Li, Y. S. Prakash, E. L. Matteson, D. J. Tschumperlin, R. Vassallo, Profibrotic effect of IL-17A and elevated IL-17RA in idiopathic pulmonary fibrosis and rheumatoid arthritis-associated lung disease support a direct role for IL-17A/IL-17RA in human fibrotic interstitial lung disease. *Am. J. Physiol. Lung Cell. Mol. Physiol.* **316**, L487–L497 (2019).
43. P. Gasse, N. Riteau, R. Vacher, M. L. Michel, A. Fautrel, F. di Padova, L. Fick, S. Charron, V. Lagente, G. Eberl, M. Le Bert, V. F. Quesniaux, F. Huaux, M. Leite-de-Moraes, B. Ryffel, I. Couillin, IL-1 and IL-23 mediate early IL-17A production in pulmonary inflammation leading to late fibrosis. *PLOS ONE* **6**, e23185 (2011).
44. R. Bernasconi, K. Thriene, E. Romero-Fernandez, C. Gretzmeier, T. Kuhl, M. Maler, P. Nauroy, S. Kleiser, A. C. Ruhl-Muth, M. Stumpe, D. Kiritsi, S. F. Martin, B. Hinz, L. Bruckner-Tuderman, J. Dengjel, A. Nyström, Pro-inflammatory immunity supports fibrosis advancement in epidermolysis bullosa: Intervention with Ang-(1-7). *EMBO Mol. Med.* **13**, e14392 (2021).
45. N. A. Evtushenko, A. K. Beilin, E. B. Dashinimaev, R. H. Ziganshin, A. V. Kosykh, M. M. Perfilov, A. L. Rippa, E. V. Alpeeva, A. V. Vasiliev, E. A. Vorotelyak, N. G. Gurskaya, hTERT-driven immortalization of RDEB fibroblast and keratinocyte cell lines followed by Cre-mediated transgene elimination. *Int. J. Mol. Sci.* **22**, 3809 (2021).
46. A. Viode, K. K. Smolen, P. van Zalm, D. Stevenson, M. Jha, K. Parker, IMPACC Network, O. Levy, J. A. Steen, H. Steen, Longitudinal plasma proteomic analysis of 1117 hospitalized patients with COVID-19 identifies features associated with severity and outcomes. *Sci. Adv.* **10**, eadl5762 (2024).
47. C. Bodemer, S. I. Tchen, S. Ghomrasseni, S. Seguier, F. Gaultier, S. Fraitag, Y. de Prost, G. Godeau, Skin expression of metalloproteinases and tissue inhibitor of metalloproteinases in sibling patients with recessive dystrophic epidermolysis and intrafamilial phenotypic variation. *J. Invest. Dermatol.* **121**, 273–279 (2003).
48. C. S. Ma, G. Y. Chew, N. Simpson, A. Priyadarshi, M. Wong, B. Grimbacher, D. A. Fulcher, S. G. Tangye, M. C. Cook, Deficiency of Th17 cells in hyper IgE syndrome due to mutations in STAT3. *J. Exp. Med.* **205**, 1551–1557 (2008).
49. L. C. Chan, S. Chaili, S. G. Filler, K. Barr, H. Wang, D. Kupferwasser, J. E. Edwards Jr., Y. Q. Xiong, A. S. Ibrahim, L. S. Miller, C. S. Schmidt, J. P. Hennessey Jr., M. R. Yeaman, Nonredundant roles of interleukin-17A (IL-17A) and IL-22 in murine host defense against cutaneous and hematogenous infection due to methicillin-resistant *Staphylococcus aureus*. *Infect. Immun.* **83**, 4427–4437 (2015).
50. J. S. Cho, E. M. Pietras, N. C. Garcia, R. I. Ramos, D. M. Farzam, H. R. Monroe, J. E. Magorien, A. Blauvelt, J. K. Kolls, A. L. Cheung, G. Cheng, R. L. Modlin, L. S. Miller, IL-17 is essential for host defense against cutaneous *Staphylococcus aureus* infection in mice. *J. Clin. Invest.* **120**, 1762–1773 (2010).
51. M. C. Marchitto, C. A. Dillen, H. Liu, R. J. Miller, N. K. Archer, R. V. Ortines, M. P. Alphonse, A. I. Marusina, A. A. Merleev, Y. Wang, B. L. Pinsker, A. S. Byrd, I. D. Brown, A. Ravipati, E. Zhang, S. S. Cai, N. Limjunyawong, X. Dong, M. R. Yeaman, S. I. Simon, W. Shen, S. K. Durum, R. L. O'Brien, E. Maverakis, L. S. Miller, Clonal $V\gamma6^+V\delta4^+$ T cells promote IL-17-mediated immunity against *Staphylococcus aureus* skin infection. *Proc. Natl. Acad. Sci. U.S.A.* **116**, 10917–10926 (2019).
52. S. Nakagawa, M. Matsumoto, Y. Katayama, R. Oguma, S. Wakabayashi, T. Nygaard, S. Saijo, N. Inohara, M. Otto, H. Matsue, G. Nunez, Y. Nakamura, *Staphylococcus aureus* virulent PSMα peptides induce keratinocyte alarmin release to orchestrate IL-17-dependent skin inflammation. *Cell Host Microbe* **22**, 667–677.e5 (2017).
53. A. Szkaradkiewicz, T. M. Karpinski, A. Zeidler, A. K. Szkaradkiewicz, H. Masiuk, S. Giedrys-Kalemba, Cytokine response in patients with chronic infections caused by *Staphylococcus aureus* strains and diversification of their Agr system classes. *Eur. J. Clin. Microbiol. Infect. Dis.* **31**, 2809–2815 (2012).
54. M. Niebuhr, M. Gathmann, H. Scharonow, D. Mamerow, S. Mommert, H. Balaji, T. Werfel, Staphylococcal alpha-toxin is a strong inducer of interleukin-17 in humans. *Infect. Immun.* **79**, 1615–1622 (2011).

55. P. P. Balraadjsing, L. D. Lund, Y. Souwer, S. A. J. Zaat, H. Frokiaer, E. C. de Jong, The nature of antibacterial adaptive immune responses against *Staphylococcus aureus* is dependent on the growth phase and extracellular peptidoglycan. *Infect. Immun.* **88**, e00733-19 (2019).
56. H. Liu, N. K. Archer, C. A. Dillen, Y. Wang, A. G. Ashbaugh, R. V. Ortines, T. Kao, S. K. Lee, S. S. Cai, R. J. Miller, M. C. Marchitto, E. Zhang, D. P. Riggins, R. D. Plaut, S. Stibitz, R. S. Geha, L. S. Miller, *Staphylococcus aureus* epicutaneous exposure drives skin inflammation via IL-36-mediated T cell responses. *Cell Host Microbe* **22**, 653–666.e5 (2017).
57. H. E. G. McWilliam, J. A. Villadangos, How MR1 presents a pathogen metabolic signature to mucosal-associated invariant T (MAIT) cells. *Trends Immunol.* **38**, 679–689 (2017).
58. C. R. Shaler, J. Choi, P. T. Rudak, A. Memarnejadian, P. A. Szabo, M. E. Tun-Abraham, J. Rossjohn, A. J. Corbett, J. McCluskey, J. K. McCormick, O. Lantz, R. Hernandez-Alejandro, S. M. M. Haeryfar, MAIT cells launch a rapid, robust and distinct hyperinflammatory response to bacterial superantigens and quickly acquire an anergic phenotype that impedes their cognate antimicrobial function: Defining a novel mechanism of superantigen-induced immunopathology and immunosuppression. *PLOS Biol.* **15**, e2001930 (2017).
59. J. E. Ussher, M. Bilton, E. Attwod, J. Shadwell, R. Richardson, C. de Lara, E. Mettke, A. Kurioka, T. H. Hansen, P. Klenerman, C. B. Willberg, $CD161^{++}$ $CD8^{+}$ T cells, including the MAIT cell subset, are specifically activated by IL-12+IL-18 in a TCR-independent manner. *Eur. J. Immunol.* **44**, 195–203 (2014).
60. M. Azzout, C. Dietrich, F. Machavoine, P. Gastineau, A. Bottier, G. Lezmi, M. Leite-de-Moraes, IL-33 enhances IFNγ and TNFα production by human MAIT cells: A new pro-Th1 effect of IL-33. *Int. J. Mol. Sci.* **22**, 10602 (2021).
61. E. Ramond, A. Lepissier, X. Ding, C. Bouvier, X. Tan, D. Euphrasie, P. Monbernard, M. Dupuis, B. Saubamea, I. Nemazanyy, X. Nassif, A. Ferroni, I. Sermet-Gaudelus, A. Charbit, M. Coureuil, A. Jamet, Lung-adapted *Staphylococcus aureus* isolates with dysfunctional agr system trigger a proinflammatory response. *J. Infect. Dis.* **226**, 1276–1285 (2022).
62. X. Ding, X. Fu, D. Euphrasie, A. Ferroni, I. Sermet-Gaudelus, A. Charbit, M. Coureuil, A. Jamet, Genomic analysis of *Staphylococcus aureus* sequential isolates from lungs of patients with cystic fibrosis. *Microbes Infect.* **25**, 105124 (2023).
63. E. Hodille, W. Rose, B. A. Diep, S. Goutelle, G. Lina, O. Dumitrescu, The role of antibiotics in modulating virulence in *Staphylococcus aureus*. *Clin. Microbiol. Rev.* **30**, 887–917 (2017).
64. H.-J. Jang, M. W. Chang, F. Toghrol, W. E. Bentley, Microarray analysis of toxicogenomic effects of triclosan on *Staphylococcus aureus*. *Appl. Microbiol. Biotechnol.* **78**, 695–707 (2008).
65. W. Chang, F. Toghrol, W. E. Bentley, Toxicogenomic response of *Staphylococcus aureus* to peracetic acid. *Environ. Sci. Technol.* **40**, 5124–5131 (2006).
66. J. M. Kwiecinski, R. M. Kratofil, C. P. Parlet, B. G. J. Surewaard, P. Kubes, A. R. Horswill, *Staphylococcus aureus* uses the ArlRS and MgrA cascade to regulate immune evasion during skin infection. *Cell Rep.* **36**, 109462 (2021).
67. P. R. Chen, S. Nishida, C. B. Poor, A. Cheng, T. Bae, L. Kuechenmeister, P. M. Dunman, D. Missiakas, C. He, A new oxidative sensing and regulation pathway mediated by the MgrA homologue SarZ in *Staphylococcus aureus*. *Mol. Microbiol.* **71**, 198–211 (2009).
68. V. Alexeev, J. C. Salas-Alanis, F. Palisson, L. Mukhtarzada, G. Fortuna, J. Uitto, A. South, O. Igoucheva, Pro-inflammatory chemokines and cytokines dominate the blister fluid molecular signature in patients with epidermolysis bullosa and affect leukocyte and stem cell migration. *J. Invest. Dermatol.* **137**, 2298–2308 (2017).
69. I. Luchsinger, N. Knöpfel, M. Theiler, M. B. des Claustres, C. Barbieux, A. Schwieger-Briel, C. Brunner, D. Donghi, M. Buettcher, B. Meier-Schiesser, A. Hovnanian, L. Weibel, Secukinumab therapy for Netherton syndrome. *JAMA Dermatol.* **156**, 907–911 (2020).
70. J. M. Fletcher, B. Moran, A. Petrasca, C. M. Smith, IL-17 in inflammatory skin diseases psoriasis and hidradenitis suppurativa. *Clin. Exp. Immunol.* **201**, 121–134 (2020).
71. J. F. Merola, R. Landewe, I. B. McInnes, P. J. Mease, C. T. Ritchlin, Y. Tanaka, A. Asahina, F. Behrens, D. D. Gladman, L. Gossec, A. B. Gottlieb, D. Thaci, R. B. Warren, B. Ink, D. Assudani, R. Bajracharya, V. Shende, J. Coarse, L. C. Coates, Bimekizumab in patients with active psoriatic arthritis and previous inadequate response or intolerance to tumour necrosis factor-α inhibitors: A randomised, double-blind, placebo-controlled, phase 3 trial (BE COMPLETE). *Lancet* **401**, 38–48 (2023).
72. A. Bardhan, L. Bruckner-Tuderman, I. L. C. Chapple, J. D. Fine, N. Harper, C. Has, T. M. Magin, M. P. Marinkovich, J. F. Marshall, J. A. McGrath, J. E. Mellerio, R. Polson, A. H. Heagerty, Epidermolysis bullosa. *Nat. Rev. Dis. Primers* **6**, 78 (2020).
73. C. C. Loh, J. Kim, J. C. Su, B. S. Daniel, S. S. Venugopal, L. M. Rhodes, L. R. Intong, M. G. Law, D. F. Murrell, Development, reliability, and validity of a novel Epidermolysis Bullosa Disease Activity and Scarring Index (EBDASI). *J. Am. Acad. Dermatol.* **70**, 89–97.e13 (2014).
74. R. R. Wick, L. M. Judd, C. L. Gorrie, K. E. Holt, Unicycler: Resolving bacterial genome assemblies from short and long sequencing reads. *PLOS Comput. Biol.* **13**, e1005595 (2017).
75. T. Seemann, Prokka: Rapid prokaryotic genome annotation. *Bioinformatics* **30**, 2068–2069 (2014).
76. V. Demichev, C. B. Messner, S. I. Vernardis, K. S. Lilley, M. Ralser, DIA-NN: Neural networks and interference correction enable deep proteome coverage in high throughput. *Nat. Methods* **17**, 41–44 (2020).
77. S. Tyanova, T. Temu, P. Sinitcyn, A. Carlson, M. Y. Hein, T. Geiger, M. Mann, J. Cox, The Perseus computational platform for comprehensive analysis of (prote)omics data. *Nat. Methods* **13**, 731–740 (2016).
78. G. Yu, L.-G. Wang, Y. Han, Q.-Y. He, clusterProfiler: An R package for comparing biological themes among gene clusters. *OMICS* **16**, 284–287 (2012).
79. W. Luo, C. Brouwer, Pathview: An R/Bioconductor package for pathway-based data integration and visualization. *Bioinformatics* **29**, 1830–1831 (2013).
80. Y. Perez-Riverol, J. Bai, C. Bandla, D. Garcia-Seisdedos, S. Hewapathirana, S. Kamatchinathan, D. J. Kundu, A. Prakash, A. Frericks-Zipper, M. Eisenacher, M. Walzer, S. Wang, A. Brazma, J. A. Vizcaíno, The PRIDE database resources in 2022: A hub for mass spectrometry-based proteomics evidences. *Nucleic Acids Res.* **50**, D543–D552 (2022).
81. M. Mempel, G. Lina, M. Hojka, C. Schnopp, H. P. Seidl, T. Schafer, J. Ring, F. Vandenesch, D. Abeck, High prevalence of superantigens associated with the egc locus in *Staphylococcus aureus* isolates from patients with atopic eczema. *Eur. J. Clin. Microbiol. Infect. Dis.* **22**, 306–309 (2003).
82. A. Jamet, J. Guglielmini, B. Brancotte, M. Coureuil, D. Euphrasie, J. Meyer, J. Roux, J. P. Barnier, E. Bille, A. Ferroni, J. F. Magny, C. Bole-Feysot, A. Charbit, X. Nassif, S. Brisse, High-resolution typing of *Staphylococcus epidermidis* based on core genome multilocus sequence typing to investigate the hospital spread of multidrug-resistant clones. *J. Clin. Microbiol.* **59**, e02454-20 (2021).

Acknowledgments: We are grateful to the National Institutes of Health Tetramer Core Facility for providing MR1 and CD1d tetramer reagents. Parts of Figs. 2A, 4A, and 6A and fig. S1C were created using templates from the Servier Medical Art (http://smart.servier.com/), licensed under a Creative Common Attribution 3.0 Generic License. We thank A. Tristan and B. Youenou of the French National Reference Centre for Staphylococci (Lyon, France) for providing AD isolates. **Funding:** This study was supported by the grant ANR (IMMUNESTA, grant no. ANR-22-CE14-0047-01, Paris, France). **Author contributions:** C.D., X.F., M.A., K.K., and N.F. performed immunoanalysis. I.M., K.R., and I.C.G. performed proteomic analysis. N.B., L.P., S.L.-M., G.L., S.H.-R., F.C.-H., and C.B. contributed to study samples and clinical data. A.J., X.F., M.D., D.E., E.U., M.M., I.D., N.M., A.F., A.C., and M.C. contributed to microbiology analysis. A.J. and M.L.-d.-M. contributed to data interpretation and discussion and supervised the study. A.C. and M.C. carefully read the manuscript. A.J., C.B., and M.L.-d.-M. wrote the manuscript. **Competing interests:** The authors declare that they have no competing interests. **Data and materials availability:** The mass spectrometry proteomics data are available via ProteomeXchange with identifier PXD049374 and dataset PXD042141 in the PRIDE repository. *S. aureus* sequences reported here are available at NCBI's BioProject database under accession number PRJNA961692. All other data associated with this study are present in the paper or the Supplementary Materials. Data from figures are in data files S2 (main text) and S3 (Supplementary Materials). All unique/stable reagents generated in this study can be provided by A.J., C.B., or M.L.-d.-M. pending a completed material transfer agreement. Requests should be submitted to anne.jamet@inserm.fr, christine.bodemer@aphp.fr, or maria.leite-de-moraes@inserm.fr.

Submitted 31 May 2024
Resubmitted 26 November 2024
Accepted 22 July 2025
Published 27 August 2025
10.1126/scitranslmed.adq7985